

THE EFFECT OF TEMPERATURE
ON BIPOLAR JUNCTION TRANSISTOR NOISE

THE EFFECT OF TEMPERATURE
ON BIPOLAR JUNCTION TRANSISTOR NOISE

By

NARENDRA K. SHAH, B.Sc. (Hons.)

A Thesis

Submitted to the School of Graduate Studies
in Partial Fulfilment of the Requirements
for the Degree
Master of Engineering

McMaster University

April 1972

ACKNOWLEDGEMENTS

The author wishes to express his deep gratitude to Dr. S.H. Chisholm for his encouragement and valuable advice during the course of this investigation. For a summer grant and most of the instruments which made this study possible, the author is grateful to the Department of Electrical Engineering and the National Research Council of Canada.

The author is much indebted to Mr. G. Kappel for his help with the transistor test circuit.

TABLE OF CONTENTS

<u>CHAPTER</u>	<u>PAGE</u>
CHAPTER 1 - INTRODUCTION	1
1.1 - Noise Studies	1
1.2 - Method	2
1.3 - Summary of the Contents	3
CHAPTER 2 - THEORY OF NOISE IN BIPOLAR TRANSISTORS	6
2.1 - Noise Sources in Silicon Planar Transistors	6
2.2 - Corpuscular Noise Theory of a BJT	10
2.3 - Base Resistance	18
2.4 - Techniques for Verification of the Theory	21
2.5 - Noise Figure of Amplifier Systems	29
CHAPTER 3 - EXPERIMENTAL RESULTS	31
3.1 - Experimental Setup and Measurement Technique	32
3.2 - Noise Spectrum Measurements	37
3.3 - Measurement of the Base Resistance	39
3.4 - Noise Figure Determination	41
3.5 - Noise Contours Plot	44
CHAPTER 4 - CONCLUSIONS	68
4.1 - Synopsis	68
4.2 - Suggestion for Further Work	69
REFERENCES	71
APPENDIX A	74
APPENDIX B	77
APPENDIX C	82
APPENDIX D	84
APPENDIX E	87
APPENDIX F	91

LIST OF ILLUSTRATIONS

<u>Figure</u>		<u>Page</u>
2.1	Groups of current carriers in an idealized n-p-n transistor in forward active region of operation.	12
2.2	Common base transistor noise equivalent circuit.	16
2.3	Cross section of an n-p-n transistor showing the base current path.	16
2.4	Modified noise equivalent circuit.	22
2.5	Transistor noise models for calculation of F.	23
3.1	Block diagram of the apparatus.	33
3.2	Test circuit to measure R_n .	34
3.3	R_n as a function of frequency.	46
3.4	R_n as a function of frequency.	47
3.5	Burst noise spectrum.	48
3.6	R_n as a function of frequency.	49
3.7	R_n' as a function of $1/T$.	50
3.8	R_n' as a function of $1/T$.	50
3.9	R_n' as a function of $1/T$.	51
3.10	R_n' as a function of $1/T$.	51
3.11	Electron mobility and resistivity as a function of $1/T$.	52
3.12	$\log_{10} r_{b'b}(T)$ as a function of $\log_{10} T$	53
3.13	R_n as a function of collector current with temperature as a parameter.	54
3.14	R_n and R_n' as a function of R_s .	55
3.15	R_n and R_n' as a function of R_s .	56
3.16	R_n and R_n' as a function of R_s .	57

<u>Figure</u>		<u>Page</u>
3.17	R_n and R'_n as a function of R_s .	58
3.18	R_n and R'_n as a function of R_s .	59
3.19	R_n and R'_n as a function of R_s .	60
3.20	R_n and R'_n as a function of R_s .	61
3.21	Noise figure contours.	62
3.22	Noise figure contours.	63
3.23	Noise figure contours.	64
3.24	Noise figure contours.	65
3.25	Noise figure contours.	66
3.26	Optimum source resistance as a function of I_c with temperature as a parameter.	67
A.1	Amplifiers in parallel for low noise input circuit.	76
B.1		81
B.2		81
B.3		81
F.1	Current gain as a function of I_c with temperature as a parameter.	93

Noise:

Any undesired sound. By extension, noise is any unwanted disturbance within a useful frequency band, such as undesired electric waves in any transmission channel or device. Such a disturbance produced by other services is called interference.

Noise is also accidental or random fluctuation in electric circuits due to motion of the current carriers. From this concept of noise, the term is used as an adjective to denote unwanted fluctuation in quantities that are desired to remain constant, or to vary in a specified manner.

Van Nostrand's Scientific
Encyclopedia (4th Edition)

CHAPTER 1

Introduction

1.1 Noise Studies

The inception of every new electron device triggers a detailed study of the various noise mechanisms in it and ways to reduce the noise¹. The bipolar junction transistor (BJT) has not been an exception to this but surprisingly enough not much work has been reported on the effect of temperature on noise and on the possibility of reducing the noise in a BJT by varying the ambient device temperature. In this thesis, the primary concern has been to investigate this aspect.

By combining the device physics and statistical analysis, the noise sources in electron devices can be well defined and characterized. The importance² of noise models and noise measurements is manifold since:

1. Noise arises from the physical mechanisms which are inherent in all semiconductor devices.
2. Noise sets the lower limit in signal detection and transmission.
3. The design for optimum signal-to-noise ratio can be achieved by coupling noise models and noise measurements.
4. Noise models and noise measurements provide other means for the determination of physical quantities such as the alpha cut-off frequency³, f_{α} , the base resistance^{4,5} of a BJT, current gain, β , the alpha cut-off frequency of a phototransistor to mention a few.
5. Noise models are powerful tools since the physical mechanisms are represented in such a way that a simple circuit theory can be

used. An example of this is the $1/f$ noise current generator representing the emitter-base surface recombination.

6. Noise measurements are helpful in predicting the life expectancy of semiconductor devices⁶.

1.2 Method

In this investigation the ambient device temperature is varied over a temperature range of -70°C (203°K) to 170°C (443°K). The criteria of these temperature limits have been that:

1. the lower limit is set by the manufacturer's specification, and
2. the upper limit for most application purposes, if not all, suffices.

The collector current range has been from $1\mu\text{A}$ to 1mA . These limits have been selected for the following reasons:

1. to assure a large current gain for signal amplification over the entire range of temperature.
2. that below $1\mu\text{A}$ not only the current gain is small but there may be some leakage current giving rise to leakage noise. However, for the family of devices under test the leakage current is of the order of nanoamperes and hence leakage noise for all practical purposes is assumed zero.

The effect of current and temperature change on the base resistance, $r_{b,b}$, of the device and subsequently on the noise performance of the device is determined to find the optimum device operating temperature.

It is to be expected that quite a few of the device parameters would be dependent on the operating conditions of current, temperature and collector voltage. Table 1.1 gives a summary of the hybrid- Π model parameters dependent of these factors. However, in the subsequent development the T-model is preferred for the following reasons:

1. hybrid- Π and T models are, after all, equivalent.
2. hybrid- Π model is inconvenient for common base applications because the current generator, $g_m V$, appears between the input and output terminals. In cases in which basewidth modulation effects are negligible the equivalent T model is more convenient for calculations¹².
3. most of the work in this field has been done on the T model²⁻⁶.

1.3 Summary of the Content

The thesis is divided into four main parts. In Chapter 2, a summary of types of noise sources is given and a noise theory of a BJT is developed. The base resistance and its dependence on current, temperature and frequency is discussed and finally the noise figure of a cascaded amplifier system is given. In Chapter 3, measurements are made to determine base resistance and its dependence on current and temperature. Measurements are also made to determine minimum noise figure's dependence on current and temperature and finally noise figure contours are plotted on R_S - I_C plane with temperature as a parameter.

In the final Chapter, conclusions of the investigations are presented.

Table 1.1

Summary of dependence of model parameters on operating condition. Except where in parentheses, statements refer to low-level injection conditions and voltages low enough for no avalanche multiplication effects.

Model Parameter†	I_c	V_c	T
g_m	$\propto I_c $ (Increases less rapidly at high currents.)	(slight increase)	$\propto 1/T$
β	Increases at moderate currents. Falls at low currents (falls at high currents).	Increases steadily. (Increases more rapidly at higher voltages, becomes infinite at sustaining voltages).	Increases steadily.
$r_{b'b}$	constant (falls at higher currents)	Increases steadily.	$\propto T^{m+2}$, for S_i and G_e $-0.3 \leq m \leq +0.7$
r_μ	$\propto 1/ I_c $ (Falls more rapidly at higher currents.)	Increases at low voltages, at higher voltages (main effect) falls due to reduction of base width (and onset of avalanche multiplication).	Approximately same as β .
r_0	$\propto 1/ I_c $	"	Insensitive
c_b	$\propto I_c $ (At higher currents: uniform base, less rapid increase; grounded base, more rapid increase.)	Reduces steadily.	$\propto 1/D_b T$ $\propto T^m$; where $+0.3 < m < +0.7$ for all Si and Ge pnp.
c_{je}	Weak increase.	Insensitive.	Insensitive

Table 1.1 (continued)

Model Parameters†	I_c	V_c	T
c_{jc}	Insensitive	$\propto V_{CB} ^n$ approximately n = 1/2 to 1/3	Insensitive
c_d	$\propto I_c $	Decreases	$\propto T^{m+1}$ (See c_b)

† Searle et. al., "Elementary Circuit Properties of Transistors", SEEC, vol. 3, page 150.

Important: All statements refer to effect of increasing $|I_c|$, $|V_c|$ or T.

CHAPTER 2

Theory of Noise in Bipolar Transistors

2.1 Noise Sources in Silicon Planar Transistors

In this section a brief introduction is given to the concept of flicker, thermal, shot and burst noise and temperature effect on them is discussed.

1. Flicker Noise:

Sometimes also referred to as excess noise or 1/f noise. It is distinguished by its peculiar spectral intensity which is of the form $\text{constant}/f^\alpha$ where α is close to unity. It occurs principally in the low-frequency region and is often negligible above 1 KHz. A number of theories have been developed to account for this 1/f behaviour. However, the most widely accepted theory is that of McWhorter and relates the flicker noise to "surface states" on the semiconducting elements⁸.

It has been shown that the flicker noise power spectrum is given by equation (2.1)

$$S(f)df = \frac{Af(T)}{f^\alpha} I^2 df \quad (2.1)$$

where A is some constant, $f(T)$ is a weak function of temperature and I is the total current flowing through the device. Experimentally, it has been found that the 1/f noise in p-n-p transistors is generally smaller than in n-p-n transistors. Also, devices built on (100) silicon

surfaces have lower noise than built on (111) surfaces. This points to the surface as the source of $1/f$ noise.

2. Thermal Noise:

It is usually caused by a random collision of carriers with the lattice, but generally found in conditions of thermal equilibrium.

Nyquist's theorem for the thermal noise of a resistance R at a temperature T gives the following expression for the available thermal noise power in a frequency interval Δf :

$$P_{av} = K T \Delta f \quad \text{where } K \text{ is Boltzmann's constant}$$

or

$$\langle e_n \rangle^2 = 4 K T R \Delta f \quad (2.2)$$

Equation (2.2) is a very important one in noise studies and it is temperature dependent. In the following work equation (2.2) will be referred to quite frequently.

3. Shot Noise:

It is caused by a random emission of electrons or photons, or a random passage of carriers across potential barriers. The spectral density of the shot noise of current i is given by the equation (2.3)

$$S_i(f) = 2qi \quad (2.3)$$

where q is the electron charge. The concept of shot noise in transistors is more thoroughly treated in section 2.2, but for the time being, it should be noted that equation (2.3) is independent of temperature.

Shot noise and thermal noise have two aspects in common. Both exhibit a flat spectrum up to a high value of frequency and both depend upon the discrete nature of charge for their generation. In generating these two types of noise the basic difference is that thermal noise is produced by the erratic movement of free charge while shot noise is produced when charge carriers suddenly appear or disappear with respect to the current that is flowing in the circuit.

4. Burst Noise:

In addition to shot, thermal, and 1/f noise, many silicon transistors, especially those of the planar-diffused type, show a type of low frequency noise known as burst noise. The noise consists typically of random pulses of variable length and equal height, but sometimes the random pulses seem to be superimposed upon each other.

It has been reported in the literature^{9,10,11} that:

- a) the equivalent input burst noise voltage e_{BB} dependence on temperature is given by the following relationship

$$e_{BB} = k_1 \exp(-T_D/T_0) \quad (2.4)$$

where T_D = device temperature, T_0 = room temperature.

- b) at constant temperature, equivalent input burst noise voltage is related to collector current by

$$e_{BB} = k_2 (I_C)^n \quad (2.5)$$

where $n \doteq \frac{1}{2}$.

The overall functional dependence of equivalent burst noise voltage upon the temperature, and base emitter voltage¹² is

$$e_{BB} = k_4 T_D^{3/2} \exp[-(E_g - qV_{BE})/2KT_D] \cdot \exp(-T_D/T_0) \quad (2.6)$$

for $n \neq \frac{1}{2}$.

The power spectrum of the burst noise has been found to be correlated⁹ to the power spectrum of a random telegraph signal. A random telegraph wave has a normalized power spectrum given by

$$S = \frac{1}{(1 + (\pi f/2a)^2)} \quad (2.7)$$

in which a is the average number of bursts per second.

These names were introduced on a more or less heuristic basis without sufficient reference to the physical causes of the noise and for this reason the following terminology has been suggested⁸.

1. Generation-recombination noise, which is caused by spontaneous fluctuations in the generation rates, recombination rates, trapping rates, etc., of the carriers, thus causing fluctuations in the free carrier densities. In bulk material the name generation-recombination noise is more appropriate than shot noise, since these carrier density fluctuations exist even if no electric field is applied. Junction devices, such as diodes and transistors operate along the principle of minority carrier injection and the applied voltage is needed to produce or change the injection level. The generation-recombination noise in these devices therefore shows much closer resemblance to shot noise than in the bulk material case.

2. Diffusion noise, caused by the fact that diffusion is a random process; consequently fluctuations in the diffusion rate give rise to localized fluctuations in the carrier density. In bulk material it is the cause of thermal noise; in junction devices it gives a major contribution to shot noise.
3. Modulation noise, which refers to noise not directly caused by fluctuation in the transition or diffusion rates which, instead, is due to carrier density fluctuations or current fluctuations caused by some modulation mechanism.

The noise sources that are temperature dependent are burst noise and thermal noise. Of these two, only the thermal noise is of importance at frequency above few KHz as burst noise is a low frequency phenomena.

2.2 Corpuscular Noise Theory of a BJT

Excellent surveys of the noise theory are given by van der Ziel^{8,13,14}, Chenette¹⁵ and Schneider and Strutt¹⁶. However, it is found from the literature that most authors on the subject follow closely the writings of van der Ziel. There are two approaches; corpuscular and collective approach, and both are equally well applicable at low injection levels for the noise in p-n junctions and transistors.

At low injection the passage of carriers across barriers can be considered as a series of independent random events. As a consequence

full shot noise should be associated with each current flowing in the device. At high frequencies the noise may be modified by transit time or diffusion time effects. This approach is called the corpuscular approach; it breaks down at high injection, since the carriers are no longer independent in that case. For many cases, however, it is a good first approximation.

The collective approach considers the noise as being caused by the random processes of diffusion and/or recombination. The noise sources to be introduced here are diffusion and generation-recombination noise sources.

However, in the following work the corpuscular approach is used. To develop it, the junction current carriers have to be investigated in greater detail. Fig. 2.1 shows the groups of current carriers in an idealized n-p-n transistor biased in the forward active region of operation. The fact that these groups of current carriers can be obtained by superimposing the "Ebers-Moll" model and "Sah-Noyce-Shockley" current of the junction makes these groups not only physically correct, but also well defined².

Initially, it is assumed that the transistor is a n-p-n unit whose d.c. characteristics are given by the Ebers-Moll relation.

$$I_E = -I_{ES} [\exp(-qV_{EB}/KT) - 1] + \alpha_R I_{CS} [\exp(-qV_{CB}/KT) - 1] \quad (2.8)$$

$$I_C = \alpha_F I_{ES} [\exp(-qV_{EB}/KT) - 1] - I_{CS} [\exp(-qV_{CB}/KT) - 1] \quad (2.9)$$

This model is quite valid for the bipolar junction transistor under test as it is operated at low injection level.

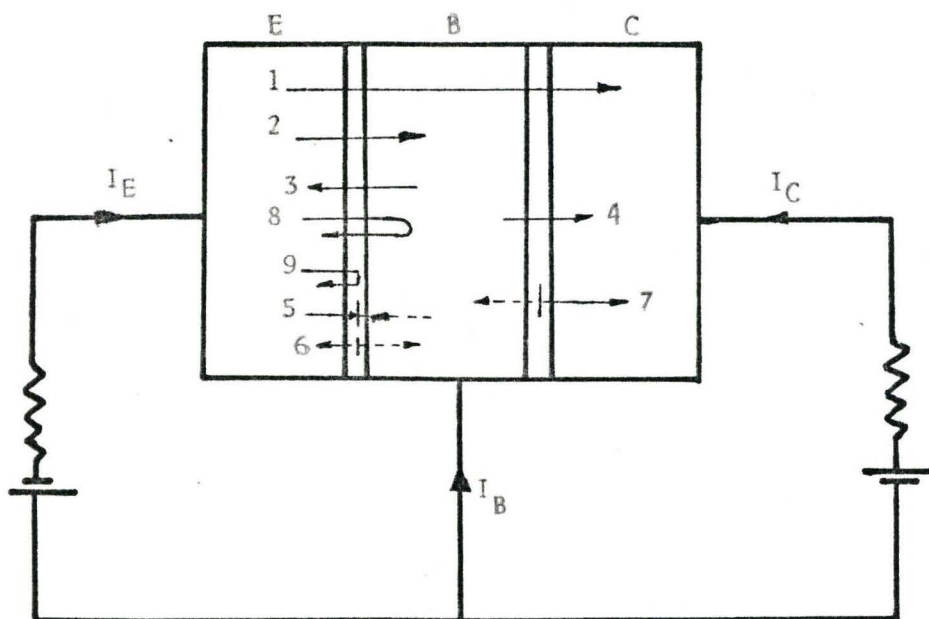


FIG. 2.1

Groups of Current Carriers in an idealized n-p-n transistor in forward active region of operation.

Table 2.1

Summary of the Various Groups of Current Carriers Shown in Fig. 2.1

Group of Carriers	Contribution To D.C. Current	Description of Carriers
1	$\alpha_F I_{ES} \exp(-qV_{EB}/KT)$	electrons emitted from the emitter into the base region and collected by the collector. This is the most important group.
2	$(1-\alpha_F) I_{ES} \exp(-qV_{EB}/KT)$	electrons emitted from the emitter into the base region and combining there.
3	$I_{ES}(1-\alpha_F)$	electrons, generated in the base region which are emitted "backwards" into the emitter.
4	$I_{CS}(1-\alpha_R)$	Electrons generated in the base region, which are collected by the collector.
5	$I_{RES} \exp(-qV_{EB}/2KT)$	Electrons emitted from the emitter towards the base but which are trapped in the transition region. They combine with the holes of group 6.
6	I_{RES}	Electrons thermally detrapped in the emitter transition region. The holes move into the base.
7	I_{RCS}	Electrons thermally detrapped in the collector transition region. The holes return to the base.
8	0	Electrons emitted into the base region but which return to the emitter. They contribute to the high frequency behaviour of the junction.
9	0	Electrons which are trapped in the emitter transition region but which are detrapped and return to the emitter.

The saturation currents I_{ES} and I_{CS} and the forward and reverse current gains, α_F and α_R , are related by the reciprocity condition

$$\alpha_F I_{ES} = \alpha_R I_{CS} \quad (2.10)$$

The Sah-Noyce-Shockley currents which result from the trapping and recombination of current carriers in the transition region are given by the formal equations

$$I_{RE} = -I_{RES} [\exp(-qV_{EB}/nKT) - 1] \quad (2.11)$$

and

$$I_{RC} = -I_{RCS} [\exp(-qV_{CB}/nKT) - 1] \quad (2.12)$$

I_{RE} and I_{RC} are the recombination currents of the emitter and collector transition regions, respectively. I_{RES} and I_{RCS} are the corresponding slightly voltage dependent "saturation currents". For the transistor biased in the forward active region $\exp(-qV_{CB}/KT) \ll 1$ and if equations (2.11) and (2.12) are added to equations (2.8) and (2.9), respectively, the d.c. characteristics are:

$$I_E = -I_{ES} \exp(-qV_{EB}/KT) + I_{ES} - \alpha_R I_{CS} - I_{RES} \exp(-qV_{EB}/nKT) + I_{RES} \quad (2.13)$$

and

$$I_C = \alpha_F I_{ES} \exp(-qV_{EB}/KT) - \alpha_F I_{ES} + I_{CS} + I_{RCS} \quad (2.14)$$

but

$$\alpha_F I_{ES} = \alpha_R I_{CS} \quad (2.10)$$

Hence, equations (2.13) and (2.14) can be written as

$$I_E = -I_{ES} \exp(-qV_{EB}/KT) + I_{ES}(1-\alpha_F) - I_{RES} \exp(-qV_{EB}/nKT) + I_{RES} \quad (2.15)$$

and

$$I_C = \alpha_F I_{ES} \exp(-qV_{EB}/KT) + I_{CS}(1-\alpha_R) + I_{RCS} \quad (2.16)$$

hence

$$I_B = I_{ES} \exp(-qV_{EB}/KT)(1-\alpha_F) + I_{RES} \exp(-qV_{EB}/nKT) - I_{ES}(1-\alpha_F) - I_{CS}(1-\alpha_R) - I_{RCS} - I_{RES} \quad (2.17)$$

Note that temperature has significant effect on the collector and emitter currents. Table 2.1 defines and describes the groups of carriers.

The representation of the noise properties of an active network by an equivalent circuit is not unique since a given circuit can be transformed into another one by applying certain network theorems. Usually one tries to find the equivalent circuit that fits closest to the physics of the device. The transistor can be characterized by two partially correlated noise sources.

The noise sources can be obtained with the help of Schottky's theorem, that is, the spontaneous fluctuations in the rate of injection and collection of minority carriers can each be represented by a shot noise current generator in parallel with the emitter-base and collector-base junctions respectively.

Hence, as shown in Fig. 2.2, which shows the low frequency noise equivalent circuit for a BJT using the common base physical T small signal model, the noise of the transistor is represented first by two current generators i_1 and i_2 , across the emitter and collector junctions respectively. The thermal noise contribution of base resistance, $r_{b'b}(T)$,

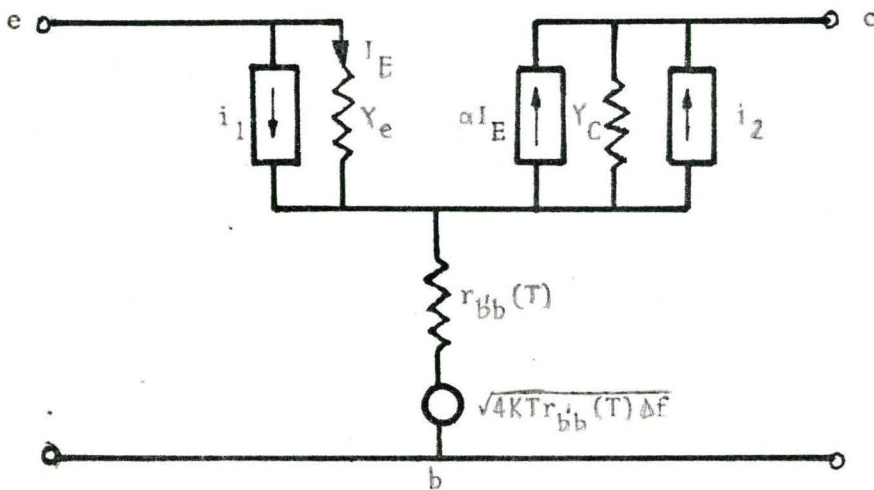


FIG. 2.2

Common Base Transistor noise equivalent circuit.

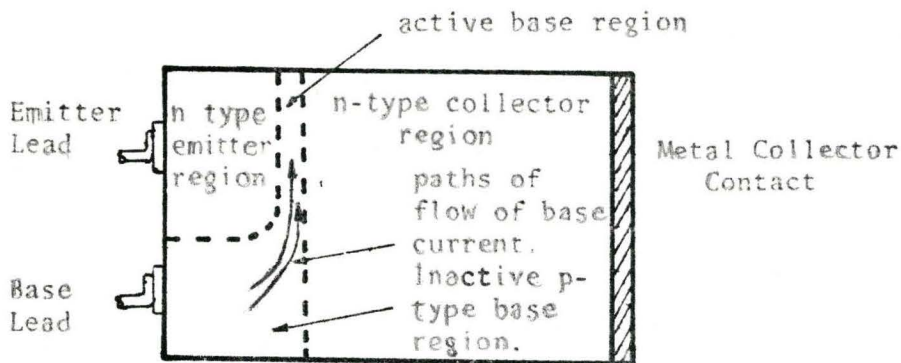


FIG. 2.3

Cross section of a npn transistor, showing the base current path.

is shown by the noise voltage generator e_b .

$$e_b = \sqrt{4KTr_{bb}(T)\Delta f} \quad \text{volts} \quad (2.18)$$

A detailed discussion on base resistance, $r_{b'b}(T_D)$ is given in section 2.3.

The current transport across the emitter-base junction results from the carriers of groups 1, 2, 3, 5 and 6. The magnitude of the shot noise contribution of these carriers is given by

$$\begin{aligned} \overline{i_1^2} &= 2q\Delta f [I_{ES} \exp(-qV_{EB}/KT) + I_{RES} \exp(-qV_{EB}/nKT) + I_{ES}(1-\alpha_F) + I_{RES}] \\ &= 2q\Delta f [I_E + 2I_{ES}(1-\alpha_F) + 2I_{RES}] \\ &= 2q\Delta f [I_E + 2I_{EE}] \end{aligned} \quad (2.19)$$

where

$$I_{EE} = I_{ES}(1-\alpha_F) + I_{RES} \quad (2.20)$$

In addition to the above sources of contribution to $\overline{i_1^2}$, the carriers of groups 8 and 9 must be included as their return to the emitter is due to a thermal process. Their contribution to $\overline{i_1^2}$ is, therefore, $4KT(g_e - g_{e0})\Delta f$. g_e represents the incremental junction conductance and g_{e0} its low frequency value. Therefore, the general expression for $\overline{i_1^2}$ becomes

$$\overline{i_1^2} = 2q\Delta f (I_E + 2I_{EE}) + 4KT(g_e - g_{e0})\Delta f \quad (2.21)$$

Similarly, the current transport across the collector-base junction results from carriers of groups 1, 4 and 7.

$$\begin{aligned}\overline{i_2^2} &= 2q\Delta f[\alpha_F I_{ES} \exp(-qV_{EB}/KT) + I_{CS}(1-\alpha_R) + I_{RCS}] \\ &= 2q\Delta f I_C\end{aligned}\quad (2.22)$$

The current generators i_1 and i_2 are strongly correlated as they have the carriers of group 1 in common. At low frequencies, the cross correlation $\overline{i_1^* i_2}$ is caused by fluctuations in this current, and has full shot noise

$$\overline{i_1^* i_2} = 2q\Delta f \alpha_F I_{ES} \exp(-qV_{EB}/KT) \quad (2.23)$$

The assumption that all current is carried by electrons is now dropped. There are then also holes going from emitter to base, from base to emitter and from the collector to base. Each of these holes contribute either to I_E or I_C , but no holes contribute to both I_E and I_C . The conditions for full shot noise again exist and equations (2.21) and (2.22) remain valid, provided that the currents ($I_E + 2I_{EE}$) and I_C are now properly redefined; for instance ($I_E + 2I_{EE}$) is now partly caused by electrons injected from the emitter into the base and partly caused by holes injected from the base into the emitter.

Note that the expressions obtained for shot noise are temperature dependent as current terms are temperature dependent.

2.3 Base Resistance, $r_{b'b}(T)$

It should be apparent that for any practical transistor geometry wherein ohmic base contact must be made around and/or along the periphery, the base current must flow parallel to the emitter and

collector junction planes as shown in Fig. 2.3. Since the base layer has a specific resistivity, this current will develop a transverse voltage drop in the base region, which appears as feedback to the emitter junction. This effect is represented by an additional term $r_{b'b}(T)$ called the base resistance.

The resistivity of the base material would be temperature dependent and hence the base resistance is temperature dependent parameter. To signify this, it is denoted by $r_{b'b}(T)$.

There are two regions of interest, the active base region under the emitter, and the inactive base region near the base contact. All the base currents must flow through the inactive region, and the current path is through material of finite conductivity. This portion of the path can be simulated by a fixed resistor in series with the base lead. It is called the extrinsic base resistance because it is outside the active region. The transverse voltage drop in the base becomes important as the current rises. Over a considerable range of current it is possible to represent the effect by an intrinsic base resistance added to the extrinsic base resistance.

The intrinsic base resistance decreases with increasing d.c. current level for two reasons. First, the strong exponential dependence of collector current on the emitter junction voltage causes the bulk of the electron current to be carried by the portion of the active region close to the base contact at high current levels. Hence, the transistor has its useful active base region narrowed at high currents and the effective resistive path length in the base is reduced. Secondly, at very high currents the low-level injection condition is

exceeded, and the excess majority-carrier concentration in the base region increases the conductivity of the base material, causing the intrinsic base resistance to drop.

At high frequencies, there can be a pronounced a.c. crowding effect in addition to d.c. crowding. The minority-carrier injection tends to be concentrated near the edges of the emitter region and this phenomenon is called emitter crowding or pinch-out. It is caused by the base current required to feed recombination. At high frequencies, the dynamic base current component which alters the base charge store can be much larger than the recombination component, and the consequent a.c. crowding can be more pronounced than the d.c. crowding. Hence, at high frequencies, only the portion of the d.c. active region near the base contact is used.

Thus, the base resistance is frequency, current and temperature dependent. However, for first approximation at low frequency and low injection level, it can be regarded as only temperature dependent.

The base resistance is a very important parameter and it is a difficult parameter to measure. Its measurement is dealt with in Chapter 3. From a d.c. point of view, the base voltage developed across the base resistance can seriously alter the action of the transistor. It affects the recombination rate in the base layer and hence the current gain of the device. Generally, low base resistance transistors have low β and high base resistance devices have high values of β . Finally, it does have an effect on the noise characteristics of the device.

2.4 Techniques for Verification of the Theory

The concept of equivalent noise resistance, R_n , is introduced and an expression for the noise factor F is derived. The theory is made general to take into account the ambient device temperature T_D .

The noise in an arbitrary transistor can always be represented by an equivalent e.m.f. e_e in series with the emitter junction and a current generator, i , in parallel with the collector junction as shown in Fig. 2.4, which is derived from the transformation of Fig. 2.2.

The equivalent noise resistance, R_n , is calculated by referring all noise sources to a single apparent e.m.f. e_n at the input of the transistor, as shown in Fig. 2.5.

$$\langle e_n^2 \rangle = 4KTR_n \Delta f \quad (2.24)$$

The noise factor, F , of the two circuits of Fig. 2.5 must be the same. There are many analogous definitions of F but to be consistent with the corpuscular model the following definition is used.

$$\begin{aligned} F &= \frac{\text{mean squared output noise current due to all sources}}{\text{mean squared output noise current due to the source}} \\ &\quad \text{resistance at room temperature}^\dagger \\ &= \overline{i_{on}^2} / \overline{i_{os}^2} \\ &= R_n / R_s \end{aligned} \quad (2.25)$$

From Fig. 2.5(b) as both circuits in Fig. 2.5 are equivalent

$$\overline{i_{on}^2} = \overline{i_{os}^2} + \overline{i_{oe}^2} + \overline{i_{oi}^2} + \overline{i_{ob}^2} \quad (2.26)$$

[†] IEEE standard room temperature is defined as $T_0=290^\circ$ but T_0 was fluctuating and hence actual room temperature is used in the definition.

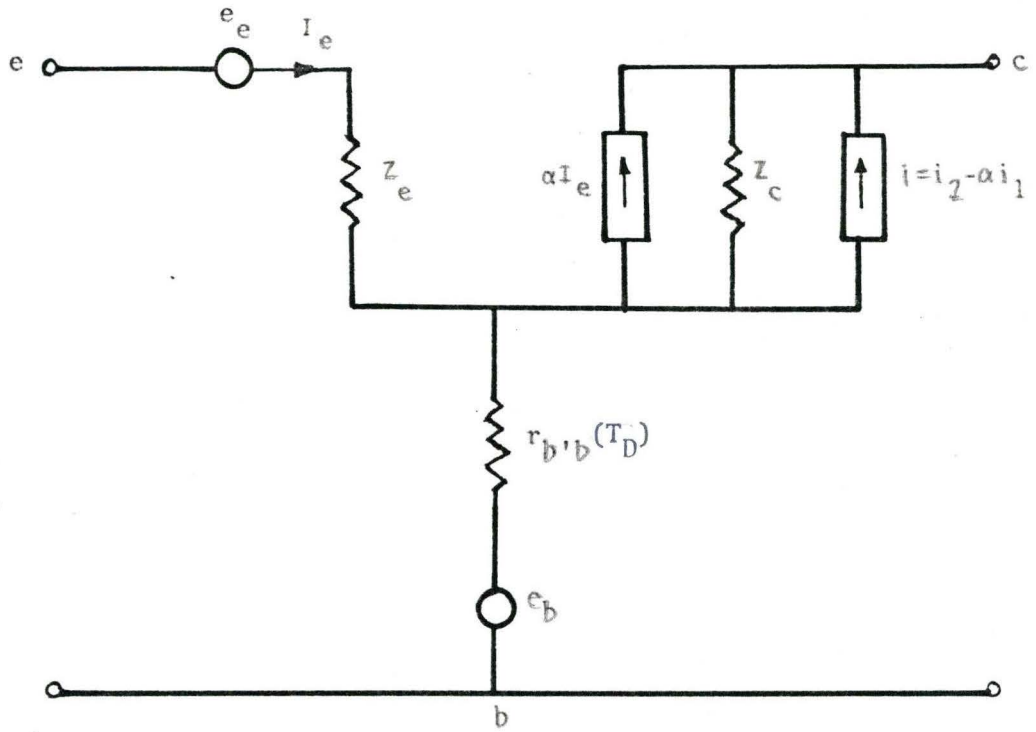
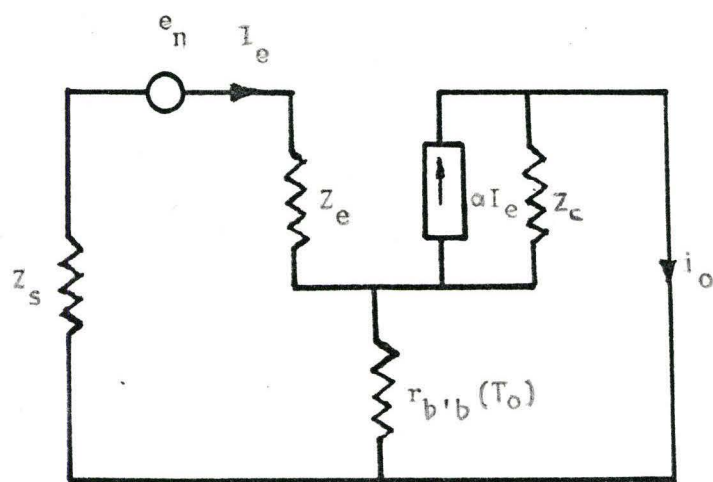
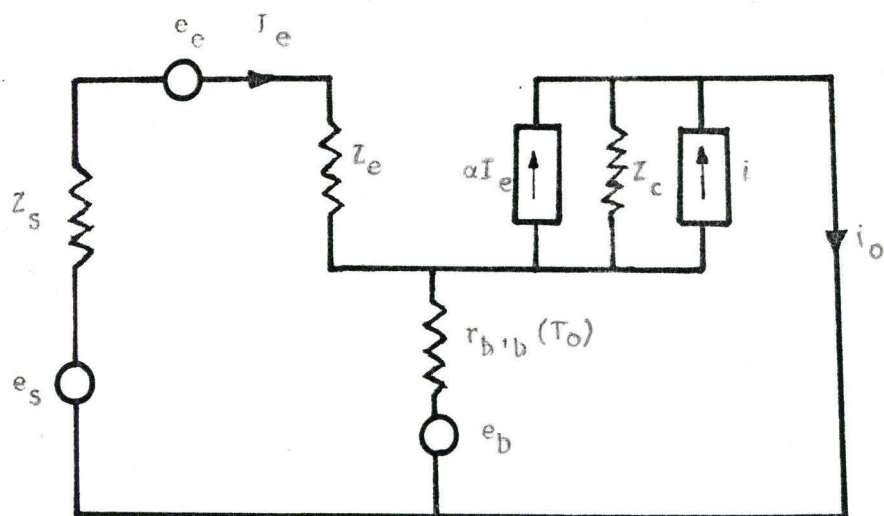


FIG. 2.4

Modified noise equivalent circuit.



(a)



(b)

FIG. 2.5

Transistor noise models for calculation of F .

substituting equation (2.26) into (2.25)

$$F = \frac{\overline{i_{os}^2} + \overline{i_{oe}^2} + \overline{i_{oi}^2} + \overline{i_{ob}^2}}{\overline{i_{os}^2}} \quad (2.27)$$

But i_{oi} and e_e are the only partially correlated noise sources and hence equation (2.27) can be simplified as

$$\begin{aligned} F &\approx 1 + \frac{\overline{i_{ob}^2}}{\overline{i_{os}^2}} + \frac{\overline{i_{oi}^2} + \overline{i_{oe}^2}}{\overline{i_{os}^2}} \\ &= 1 + \frac{r_{b'b}(T_o)}{R_s} + \frac{\overline{i_{oi}^2} + \overline{i_{oe}^2}}{\overline{i_{os}^2}} \end{aligned} \quad (2.28)$$

where $r_{b'b}(T_o)$ is the base resistance at room temperature. From Fig. 2.5(b)

$$i_{oe} = \frac{\alpha e_e}{Z_e + Z_s + (1-\alpha)r_{b'b}(T_o)} \quad (2.29)$$

$$i_{os} = \frac{\alpha e_s}{Z_e + Z_s + (1-\alpha)r_{b'b}(T_o)} \quad (2.30)$$

and

$$i_{oi} = \frac{i(Z_e + Z_s + r_{b'b}(T_o))}{Z_e + Z_s + (1-\alpha)r_{b'b}(T_o)} \quad (2.31)$$

Hence

$$\frac{\overline{i_{oi}^2} + \overline{i_{oe}^2}}{\overline{i_{os}^2}} = \frac{(\alpha e_e + iZ_{tot})^2}{|\alpha|^2 e_s^2} \quad (2.32)$$

where

$$Z_{tot} = Z_e + Z_s + r_{b'b}(T_o) \quad (2.33)$$

Arbitrary values are assigned to e_e and i and four noise parameters are introduced³; the noise conductance, $g_{s\ell}$, the noise resistance, $r_{s\ell}$, and the correlation impedance $Z_{sc} = R_{sc} + jX_{sc}$. Initially, e_e is split into a part e_e'' uncorrelated with i , and a part e_e' fully correlated with i . The noise parameters are defined as

$$\frac{\overline{i^2}}{|\alpha|^2} = 4KT_0 g_{s\ell} \Delta f \quad (2.34)$$

$$\begin{aligned} Z_{sc} &= R_{sc} + jX_{sc} \\ &= \frac{\alpha e_e'}{i} = \frac{\overline{\alpha e_e' i^*}}{i i^*} = \frac{\overline{\alpha e_e i^*}}{i^2} \end{aligned} \quad (2.35)$$

$$\begin{aligned} \overline{e_e''^2} &= 4KT_0 r_{s\ell} \Delta f = \overline{e_e^2} - \overline{e_e'^2} \\ &= \overline{e_e^2} - \frac{\overline{i^2} |Z_{sc}|^2}{|\alpha|^2} = \frac{\overline{e_e^2 i^2} - (\overline{e_e^* i})^2}{i^2} \end{aligned} \quad (2.36)$$

Hence, equation (2.32) can be written as

$$\begin{aligned} \frac{(\overline{\alpha e_e + i Z_{tot}})^2}{|\alpha|^2 \overline{e_s^2}} &= \frac{(\overline{\alpha e_e' + \alpha e_e'' + i Z_{tot}})^2}{|\alpha|^2 \overline{e_s^2}} \\ &= \frac{\overline{i^2}}{|\alpha|^2} \frac{|Z_{sc} + Z_{tot}|^2}{\overline{e_s^2}} + \frac{\overline{e_e''^2}}{\overline{e_s^2}} \end{aligned} \quad (2.37)$$

Therefore, the noise figure F is given by

$$F = 1 + \frac{r_{b'b}(T_0)}{R_s} + \frac{r_{s\ell}}{R_s} + \frac{g_{s\ell}}{R_s} |Z_{sc} + Z_e + Z_s + r_{b'b}(T_0)|^2 \quad (2.38)$$

Combining equations (2.25) and (2.38), the equivalent noise resistance, R_n , is obtained as

$$R_n = R_s + r_{sl} + r_{b'b}(T_o) + g_{sl} |Z_s + Z_e + r_{b'b}(T_o) + Z_{sc}|^2 \quad (2.39)$$

Consider this quantity as a function of Z_{sc} and let

$$Z_e = r_e + jX_e$$

$$Z_{sc} = R_{sc} + jX_{sc}$$

$$Z_s = R_s + jX_s \quad (2.40)$$

It may be seen that R_n , as a function of X_s is a minimum at

$$X_s + X_e + X_{sc} = 0 \quad (2.41)$$

At low frequency this is so. Hence, at the minimum value of R_n

$$R_n = R_s + r_{sl} + r_{b'b} + g_{sl} [R_s + r_e + R_{sc} + r_{b'b}(T_o)]^2 \quad (2.42)$$

which can be written as

$$R_n = A + BR_s + CR_s^2 \quad (2.43)$$

where

$$A = r_{sl} + r_{b'b}(T_o) + g_{sl} [r_e + R_{sc} + r_{b'b}(T_o)]^2$$

$$B = 1 + 2g_{sl} [r_e + R_{sc} + r_{b'b}(T_o)]$$

$$C = g_{sl} \quad (2.44)$$

Note that equation (2.43) is a quadratic equation and hence measurement of R_n as a function of R_s will generate points that belong

to a quadratic function. Subsequently, coefficients A, B and C and hence $g_{s\ell}$, $r_{b'b}(T_0)$ and $r_{s\ell}$ can be determined from the shape of the curve.

In the derivation of equation (2.43) the ambient device temperature was that of the room temperature. However, this expression has to be modified if the ambient device temperature is T_D . In equation (2.42) multiplying each equivalent noise resistance element by the appropriate 'elemental' temperature, equation (2.42) becomes

$$4KT_D R_n \Delta f = 4KT_0 R_s \Delta f + 4KT_D r_{s\ell} \Delta f + 4KT_D r_{b'b}(T_D) \Delta f + 4KT_D g_{s\ell} |R_s + r_e + R_{sc} + r_{b'b}(T_D)|^2 \quad (2.45)$$

where T_0 is room temperature.

If we let

$$4KT_D R_n \Delta f = 4KT_0 R_s \Delta f + 4KT_D R'_n \Delta f \quad (2.46)$$

The transistor equivalent noise resistance R'_n is defined as

$$R'_n = r_{b'b}(T_D) + r_{s\ell} + g_{s\ell} |R_s + r_e + r_{b'b}(T_D) + R_{sc}|^2 \quad (2.47)$$

Hence R'_n can be expressed as

$$R'_n = A' + B'R_s + C'R_s^2 \quad (2.48)$$

where

$$A' = r_{b'b}(T_D) + r_{s\ell} + [g_{s\ell} |r_e + r_{b'b}(T_D) + R_{sc}|^2]$$

$$B' = 2g_{s\ell} [r_{b'b}(T_D) + r_e + R_{sc}]$$

$$C' = g_{s\ell} \quad (2.49)$$

To a first approximation the terms in the bracket can be neglected, as $g_{s\ell}$ is of the order of 10^{-4} .

From equation (2.46)

$$R'_n = R_n - \frac{T_o R_s}{T_D} \quad (2.50)$$

From equation (2.48), it is noted that the relation between R'_n and R_s is quadratic and that R'_n can be easily obtained from the measurement of the equivalent noise resistance R_n as a function of the source resistance R_s as given by equation (2.50).

Theoretically, R_{sc} is zero at low frequency³ and passes through a maximum for higher frequencies. $r_{s\ell}$ would be of the order of $\frac{r_e}{2}$ at low frequencies and should decrease rapidly with increasing frequency. r_e is given as

$$r_e = \frac{KT}{q} \frac{1}{I_E} = \frac{KT}{q} \frac{1}{I_C} \quad (\text{for high } \beta_o) \quad (2.51)$$

It can easily be shown that to a good approximation this is valid.

Thus, the equation (2.47) is temperature dependent.

So far, in the development of the above theory F 's dependence on frequency has not been brought out. This is primarily due to the fact that above $1/f$ region F is independent of frequency up to about 1 MHz. However, Nielsen¹⁷ has obtained an expression for F dependent on frequency as

$$F = 1 + \frac{r_{b'b}(T_D)}{R_s} + \frac{r_e}{2R_s} + \frac{(1-\alpha_o)(1+f/\sqrt{(1-\alpha)}f_\alpha)^2 (R_s + r_{b'b}(T_D) + r_e)^2}{2\alpha_o r_e R_s} \quad (2.52)$$

In this derivation a good agreement between theory and experiment was obtained by neglecting correlation (that is, putting $Z_{sc}=0$) and taking

$$r_{sl} = \frac{1}{2} r_e \quad (2.53)$$

f_α is the α cutoff frequency.

At low frequency equation (2.53) simplifies to

$$F = 1 + \frac{r_{b'b}(T_D)}{R_s} + \frac{r_e}{2R_s} + \frac{(R_s + r_{b'b}(T_D) + r_e)^2}{2\beta_o r_e R_s} \quad (2.54)$$

where β_o is the common emitter current gain.

2.5 Noise Figure of Cascaded Amplifier Systems

So far, the development has been to determine the noise figure of a single device but in practice a system of devices rather than a single device is used. Nevertheless, it is found that it is the first transistor stage that has the most significant effect on the overall noise figure. The overall noise figure F is given as⁷

$$F = F_1 + \frac{F_2 - 1}{G_1} + \frac{F_3 - 1}{G_1 G_2} + \dots \quad (2.55)$$

where

F_1 = noise factor of 1st stage

F_2 = noise factor of 2nd stage

F_3 = noise factor of 3rd stage

G_1 = available power gain of 1st stage

G_2 = available power gain of 2nd stage

The overall equivalent noise resistance R_N is given by the analogous equation

$$R_N = R_{N1} + \frac{R_{N2}}{A_1^2} + \frac{R_{N3}}{(A_1 A_2)^2} \quad (2.56)$$

where

R_{N1} = equivalent noise resistance of 1st stage

R_{N2} = equivalent noise resistance of 2nd stage

R_{N3} = equivalent noise resistance of 3rd stage

A_1 = available voltage gain of 1st stage

A_2 = available voltage gain of 2nd stage

Hence, from equations (2.55) and (2.56), it is the 1st stage of the system that dominates and influences the overall noise performance of the amplifier system. Subsequently, in Chapter 3, we are concerned with the investigation of the noise dependence on temperature of the first stage only.

Faulkner¹⁸ has developed a technique of amplifiers connected in parallel to reduce the overall noise figure of the system. This technique is illustrated in Appendix A.

CHAPTER 3

Experimental Results

Experimental measurements on a bipolar junction low level low noise diffused silicon planar transistor were carried out to determine the equivalent noise resistance as a function of temperature and collector current. The base resistance's dependence on temperature and collector current is determined from these measurements. R_n is measured as a function of source resistance with temperature and collector current as parameters. The minimum noise figure as a function of temperature and current is obtained from these measurements.

Noise figure contours are plotted in the R_s-I_c plane using Nielsen's formula, equation (2.54). From these contours, the optimum source resistance and hence optimum noise figure at a given operating condition is determined.

In the following work, most of the noise measurements are done in terms of equivalent noise resistance R_n as opposed to noise factor as a figure of merit¹⁹ for the following reasons:

- 1) it is easier to measure, and
- 2) the highest (or best) signal-to-noise ratio is obtained with a lowest value of R_n , whereas the noise factor only indicates the degree to which the signal-to-noise ratio is degraded by the transistor. The lowest noise factor does not necessarily correspond to the highest signal-to-noise ratio at the output.

3.1 Apparatus

A block diagram of the measuring system for low and medium frequency is shown in Fig. 3.1.

There are many requirements to meet to assure a correct noise measurement of the system. The essential equipment needed is

- 1) a low noise linear amplifier which is able to amplify the noise in the desired frequency band to a level high enough to be detected.
- 2) a wide range sinusoidal signal generator with a calibrated output for gain calibration and system tuning purposes.
- 3) an oscilloscope for monitoring purposes.
- 4) a quadratic detector of which the output is proportional to the amplifier output power (or a linear detector with an output proportional to the square root of the noise power detected).
- 5) the bandwidth of the amplifier system should be greater than the frequency range under investigation.

Fig. 3.2 shows the actual transistor test setup used for the low and medium frequency noise measurement. The test transistor, referred to as TUT, is connected in a common emitter configuration with its output directly connected to another transistor in the common base connection.

It can easily be calculated, as shown in Appendix B, that if the common-base transistor has the same characteristics as the test transistor, it does not contribute measurably to the overall noise.

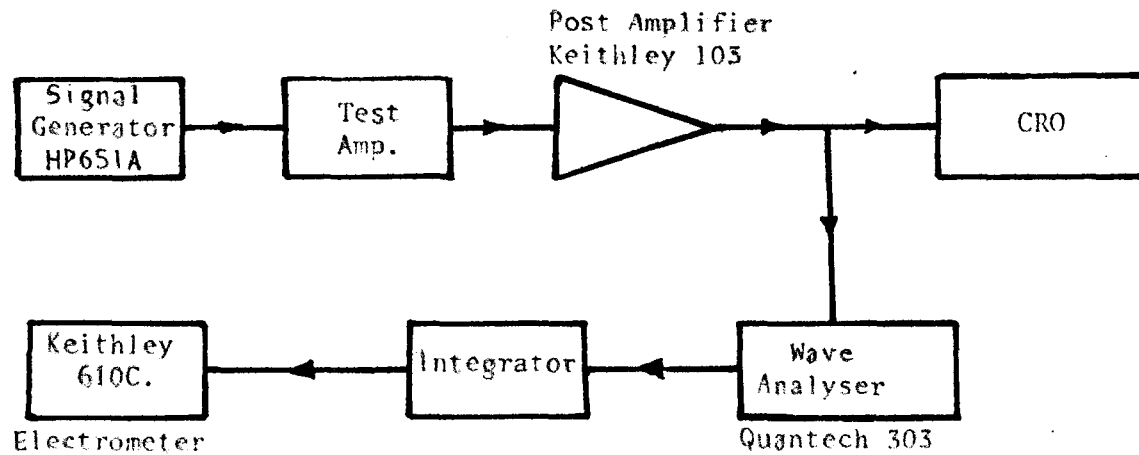


FIG. 3.1

Block diagram of the apparatus.

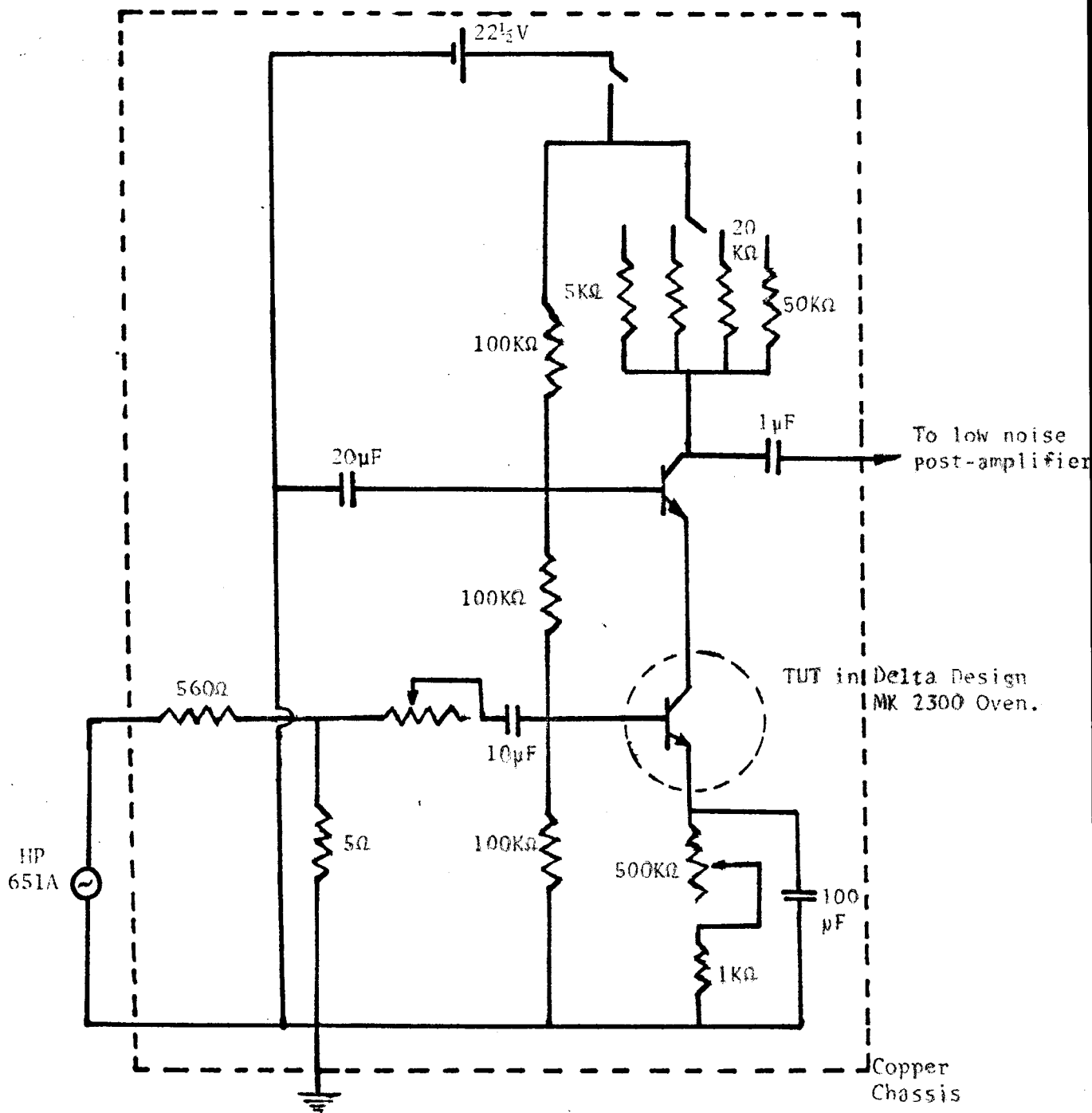


FIG. 3.2

Test circuit to measure R_n .

A number of points on the choice of the above configuration are:

- 1) The common emitter circuit has both voltage gain and current gain while the common base circuit has voltage gain but current gain is less than 1. Hence, the cascaded arrangement is advantageous in boosting both current and voltage amplification of the signal at the common-emitter input.
- 2) the collector current and voltage gain of the system can be varied independently,
- 3) component values of R and C's were selected to give the operating current range as well as amplifier system midbandwidth from about 20 Hz to about 20 KHz.

The basic difficulty in measuring the device noise was to eliminate the ground loops and to minimize the background noise level. In Appendix C, an outline is given as to the steps taken to avoid these pitfalls. The background noise level was less than 1 percent of the device noise power level and in subsequent calculations this noise contribution was neglected.

Hence, the measurement philosophy had been that the noise power measured at the output was solely due to the device under test and knowing the voltage gain of the amplifier system, the equivalent noise resistance at the input of the transistor was calculated using equation (2.24). Subsequently, the following technique was adapted for determination of the equivalent noise resistance, R_n .

- 1) The desired bias voltage is applied to the TUT with the collector current being monitored to ensure that no drift occurred. The

collector-emitter voltage drop, V_{CE} , was kept at about 2.7V and a slight variation in this value of V_{CE} was found to have negligible effect on the collector current or the signal output.

- 2) The voltage gain G_V of the system is determined by applying a small signal voltage at the frequency of interest to the output of TUT as shown in Fig. 3.2. The input and output signals are measured on the HP 3400A voltmeter to determine the voltage gain of the system:
- 3) The equivalent noise bandwidths of the Quantech Wave Analyser model 303 were taken to be the values of the 3 db signal power bandwidths. The bandwidth was progressively increased from 10,30,100 to 1,000 Hz with increasing frequency.
- 4) The ambient device temperature was controlled by having it in a Delta Design oven type MK 2300. The coolant used was liquid nitrogen.

It is believed²⁰ that the relative noise measurements are accurate within 5 percent and the absolute noise measurements are accurate within 10 percent. The main source of errors in these types of measurements is due to fluctuations in the rectified noise power reading on the wave analyser and hence, a voltage integrator is used to average out these fluctuations. However, the measurement accuracy and limitations are discussed in Appendix D.

3.2 Noise Spectrum Measurements

To ensure that all measurements were performed well above 1/f noise region, it has initially to be determined. The 1/f noise region's dependence on temperature and current is investigated. Initially, the current is kept constant and the ambient device temperature is varied as shown in Figs. 3.3 to 3.5. At low temperature burst noise was present and this is discussed later in the section. However, above room temperature 1/f noise region was not noticeably affected by temperature change. This type of behaviour is to be expected from equation (2.1) as $f(T)$ is a weak function of temperature. The magnitude of the 1/f noise is dependent on the current flowing through the device as can be seen from Figs. 3.3 and 3.6.

In absence of the burst noise, the "corner" frequency is independent of the ambient device temperature and the current flowing through the device. The "corner" frequency is defined as the intersection of the 1/f slope and the frequency independent noise level.

The "corner" frequency obtained is about 150 Hz, that is the 1/f noise region is up to 150 Hz. There is some discrepancy of values of the 1/f region obtained by others working on the same family of transistors. This is illustrated in Table 3.1.

The discrepancy with Martin et. al. can only be explained on the basis that their device had an additional gate and probably processed by a different manufacturer. The values obtained in this investigation are in fair agreement with the ones given by Fairchild. Fairchild gives the "corner" frequency as being dependent on I_C and R_S , however, this was not so for $R_S < 1000$ ohms.

Table 3.1

<u>Transistor type</u>	<u>Author</u>	<u>1/f region</u>	<u>T°K</u>	<u>I_c (μA)</u>	<u>R_s (Ω)</u>
2N2484	Martin et. al ^{2,1}	10 Hz	300		
2N2484	Fairchild	< 2 KHz	300	1000	1000
2N2484	Shah	~ 120 Hz	303	600	500
2N2484	Shah	~ 140 Hz	373	600	500
2N930	Roig ²	~ 200 KHz	77		

Burst noise was present at temperatures below -30°C (243°K). A typical burst noise spectrum is shown in Fig. 3.5 and shows $1/f^2$ dependence of burst noise as predicted from equation (2.7).

It was found during measurements that burst noise is a decreasing function of device temperature and a function of the collector current as predicted by equations (2.4) and (2.5). The pulse width and the pulse repetition rate of the burst noise was found to fluctuate randomly. Repeated cyclic heating and cooling of the TUT from 443°K to 203°K had the effect of reducing the burst noise pulse width if not eliminating this particular type of noise.

The temperature effect on the burst noise suggests that perhaps it is associated with recombination centres. However, many theories and models have been proposed to explain this switching behaviour of the burst noise^{9,10,11,22}, but it is still in the investigative stage. The burst noise measurements are made difficult as it has a non-Gaussian distribution.

3.3 Measurement of Base Resistance

The importance of the base resistance, $r_{b'b}(T)$, was discussed in section 2.3 and it is one of the transistor parameters that is not easily measured. This is because it is the real part of a complex distributed impedance which is in series with the emitter-base diode. However, a number of techniques have been developed to determine $r_{b'b}(T)$ and Appendix E gives a brief survey of some of the methods available to find $r_{b'b}(T)$. However, each technique may be applicable only to a particular class of devices.

Method.1:

For low source resistance, $R_s < 10$ ohms, from equation (2.48)

$$R'_n = r_{b'b}(T) + r_{s\ell} = r_{b'b}(T) + \frac{1}{2} r_e \quad (3.1)$$

$$r_{b'b}(T) = R'_n - \frac{1}{2} r_e \quad (3.2)$$

That is, from the knowledge of R'_n at various operating conditions of current and temperature, the base resistance can be calculated.

R'_n was determined at a frequency well above 1/f noise region, at 2KHz, as shown in Figs. 3.7 to 3.10 over a temperature range of 170°C to -70°C, (443°K, 203°K), with collector current as a parameter.

$r_{b'b}(T)$ was found to be current independent but temperature dependent. This would be expected to be so from the discussion of section 2.3. The increase of $r_{b'b}(T)$ with increasing temperature is primarily due to a decrease of the carrier mobility with increasing temperature²². Fig. 3.11 shows the electron mobility and relative

resistivity as a function of temperature. $r_{b'b}(T)$'s dependence on temperature is analogous to the relative resistivity's dependence on temperature.

For low temperatures, base resistance is a gradually increasing function of temperature, but for $T \geq 250^\circ\text{K}$, $r_{b'b}(T)$ is proportional to $T^{1.9}$ as shown in Fig. 3.12. This value obtained is within the range of values predicted from Table 1.1.

Method 2:

This technique is rather a crude one to measure $r_{b'b}(T)$. From equations (2.54) and (2.25) the relation between R_n and I_C is some form of a quadratic. Combining equations (2.54) and (2.25), equation (3.3) is obtained

$$\begin{aligned} R_n &= R_s + r_{b'b}(T) + \frac{r_e}{2} + \frac{(R_s + r_{b'b}(T) + r_e)^2}{2\beta_o r_e} \\ &= R_s + r_{b'b}(T) + \frac{KT}{2q} \frac{1}{I_C} + \frac{(R_s + r_{b'b}(T) + \frac{KT}{q} \frac{1}{I_C})^2}{2\beta_o \frac{KT}{q} \frac{1}{I_C}} \end{aligned} \quad (3.3)$$

Differentiating w.r.t. I_C and multiplying by I_C yields

$$\frac{dR_n}{dI_C} \cdot I_C = \frac{-KT}{2qI_C} + \frac{(R_s + r_{b'b}(T) + \frac{KT}{q} \cdot \frac{1}{I_C})^2}{2\beta_o \frac{KT}{qI_C}} - \frac{(R_s + r_{b'b}(T) + \frac{KT}{q} \cdot \frac{1}{I_C})}{\beta_o} \quad \dots (3.4)$$

At a minimum this is zero and hence from equation (3.3) and equation

(3.4)

$$R_n - \frac{dR_n}{dI_C} \cdot I_C = R_s + r_{b'b}(T) + \frac{KT}{q} \cdot \frac{1}{I_C} + \frac{R_s + r_{b'b}(T) + \frac{KT}{q} \cdot \frac{1}{I_C}}{\beta_o} \quad (3.5)$$

For small R_s and $\beta_o \gg 1$

$$R_{n_{\min}} = r_{b'b}(T) + r_e$$

That is

$$r_{b'b}(T) = R_{n_{\min}} - r_e \quad (3.6)$$

The results obtained were as shown in Fig. 3.13 and the value of the base resistance obtained is in a good agreement with the ones obtained by method 1 as shown in Table 3.2.

Table 3.2

<u>Method 1 (Ω)</u>	<u>Method 2 (Ω)</u>	<u>Temperature ($^{\circ}\text{K}$)</u>
250	260	223
350	332	273
440	408.5	313
650	612	373

3.4 Noise Figure

In this section, F 's dependence on temperature and current is investigated.

1. Dependence on Temperature

In equation (2.48) it has been shown that R'_n is a quadratic function of R_s . For easy reference the equation is repeated here

$$R'_n = A' + B'R_s + C'R_s^2 \quad (2.48)$$

From the shape of the characteristics, the coefficients A' , B' and C' can easily be determined.

Hence, F can be written as

$$F = \frac{T_0 R_s + T_D R_n'}{T_0 R_s}$$

$$= 1 + T_D/T_0 (A'/R_s + B' + C'R_s) \quad (3.7)$$

Differentiating w.r.t. R_s gives

$$\frac{dF}{dR_s} = 0 \quad \text{at} \quad R_s^2 = \frac{A'}{C'}$$

Hence

$$F_{\min} = 1 + \frac{T_D}{T_0} (B' + 2\sqrt{A'C'}) \quad (3.8)$$

The equivalent noise resistance was determined as a function of the source resistance with temperature as a parameter, keeping I_c constant. Figs. 3.14 - 3.18 show that R_n' is almost constant up to $R_s = 500\Omega$. The meaningful interpretation of this is that the signal-to-noise ratio is least degraded by the transistor noise in this region.

The minimum noise figure is calculated from equation (3.8) and the temperature effect on it is shown in Table 3.3.

Table 3.3

F_{\min}	$T(^{\circ}\text{K})$
1.59	253
1.69	303
1.86	348
2.45	393
2.85	433

Table 3.3 clearly shows that the noise figure is degraded as temperature is increased. Intuitively, as $r_{b,b}(T)$ is an increasing function of temperature, its eventual effect on the noise performance of the device under test is to degrade it as temperature is increased. The degradation of F_{\min} over a temperature range of 253°K to 433°K is approximately 2.5 db hence there is a definite advantage to operate the device at lower temperatures. However, at temperatures less than 243°K burst noise may be present and due to its unpredictable nature the operation of the device below this temperature is inadvisable, especially when reliable noise performance is required at low frequency.

2. Dependence on Collector Current

The noise figure is a function of current as shown in Chapter 2. Using similar techniques as in the last section, R'_n was determined as a function of R_s , with the collector current as a parameter at a constant temperature. The characteristics obtained are similar to the temperature ones as shown in Figs. 3.15, 3.19, 3.20. Table 3.4 makes a comparison of the values obtained.

Table 3.4

F_{\min}	I_C (μ A)
1.69	650
1.49	350
1.48	54

As expected, F_{\min} decreases with decreasing I_C , however, this is not a desirable way of reducing F_{\min} as the current gain decreases with decreasing I_C .

3.5 Noise Figure Contours

It is a usual practice for a manufacturer to give contours of a constant noise figure in the I_C - R_S plane. However, these contours are usually determined only at room temperature. In this section, these contours are evaluated using Nielsen's simplified equation (2.54) over a temperature range of 223°K to 433°K.

Rewriting equation (2.54) as a quadratic equation in the unknown R_S provides a convenient means for determining the range of source resistance over which the noise factor of the amplifier will be less than or equal to a specified value

$$R_S^2 + R_S [2(r_{b,b}(T) + r_e) - 2\beta_o r_e (F-1)] + (r_{b,b}(T) + r_e)^2 + 2\beta_o r_e [r_{b,b}(T) + \frac{r_e}{2}] = 0 \quad (3.9)$$

This expression is graphically presented in Figs. 3.21 - 3.25 for values of noise factor, F , under the stipulation that $r_{b,b}(T)$ is independent of current and its value used is determined from previous measurement. The current gain β_o is a function of I_C and is measured on a Tektronix curve tracer Type 576 as shown in Appendix F.

The single line curve marked R_{sopt} which intersects the contours of constant noise factor, is the variation of the optimum value of source resistance with operating point. The optimum value of the noise factor can only be obtained when the device is driven with its optimum value of source resistance, R_{sopt} . The effect of increasing temperature is to increase this optimum source resistance R_{sopt} as shown in Fig. 3.26. Using the known value of the optimum source resistance at a given operating current and temperature, the optimum noise factor, F_{opt} , is calculated from equation (2.54). The value of F_{opt} obtained by this

method is compared to the one obtained from section 3.4.1 in Table 3.5.

Table 3.5

<u>F_{min}</u>	<u>F_{opt}</u>	<u>T°K</u>	<u>I_C (μA)</u>
1.59	1.26	253	640
1.69	1.26	303	650
1.86	1.25	348	650
2.45	1.25	393	650
2.85	1.25	433	660

Hence, F_{opt} is within 0.03 db over temperature range 253°K to 433°K, that is constant. It can easily be seen from the noise figure contours that I_C decreasing has the effect of increasing, R_{sopt} and subsequently reducing F_{opt} . That is, F_{opt} can be reduced by lowering the collector current but as mentioned earlier this is not desirable as β_o falls with decreasing current.

There is a wide discrepancy between F_{min} and F_{opt} values obtained. Both were derived using different techniques and the values of R_s at F_{min} and F_{opt} conditions are different. F_{opt} obtained would be that of the "ideal" condition whereas F_{min} is obtained from the value of R_s in Figs. 3.14 - 3.18 at which R'_n has the minimum in the characteristics. Taking these values of R_s at R'_n minimum and substitute for R_s at given operating temperature and current conditions the values of F obtained from the noise figure contours are in good agreement with F_{min} in Table 3.5.

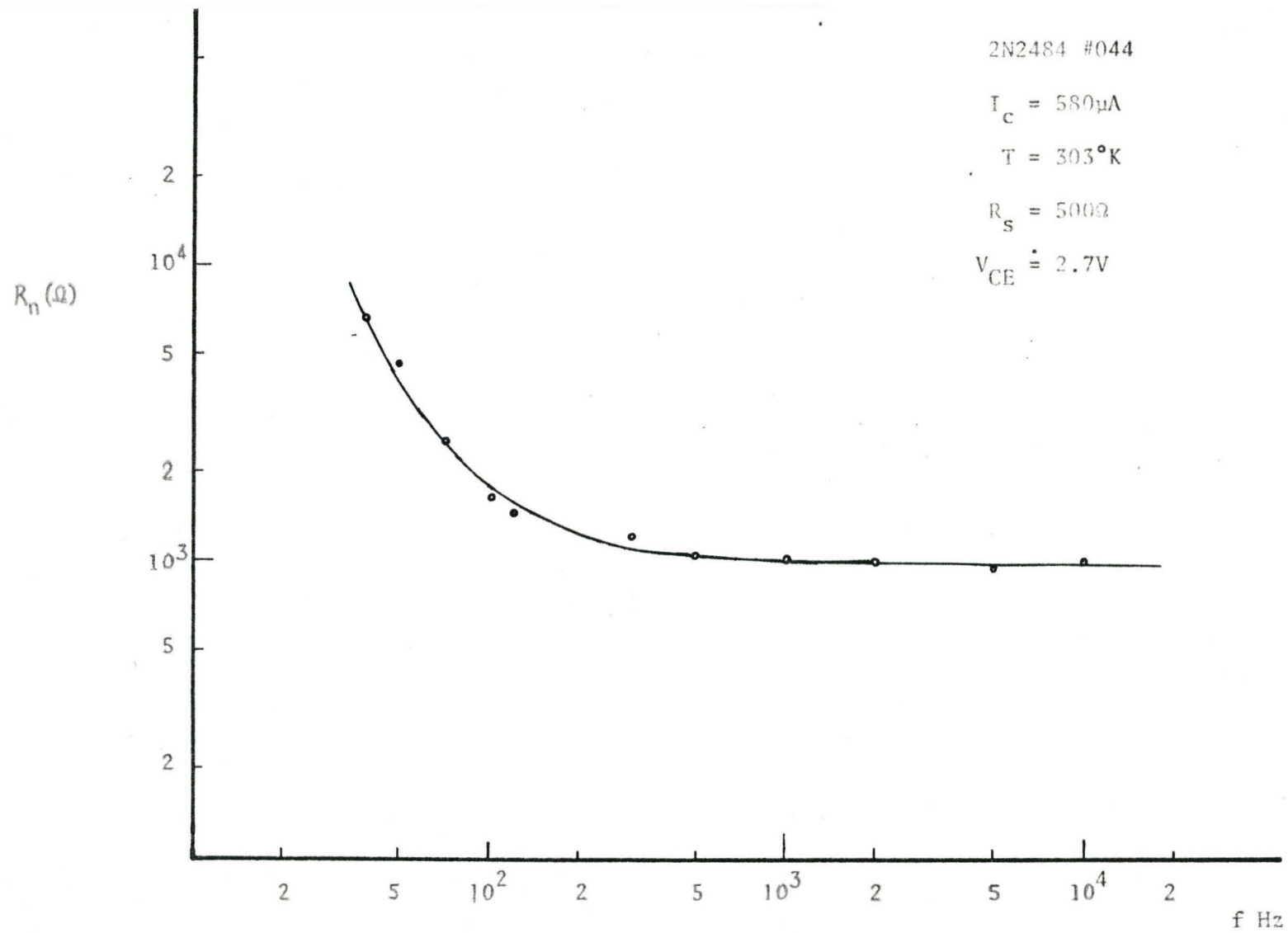


FIG. 3.3

R_n as a function of frequency.

2N2484 #044
 $I_C = 610\mu A$
 $T = 373^\circ K$
 $R_S = 500\Omega$
 $V_{CE} = 2.7V$

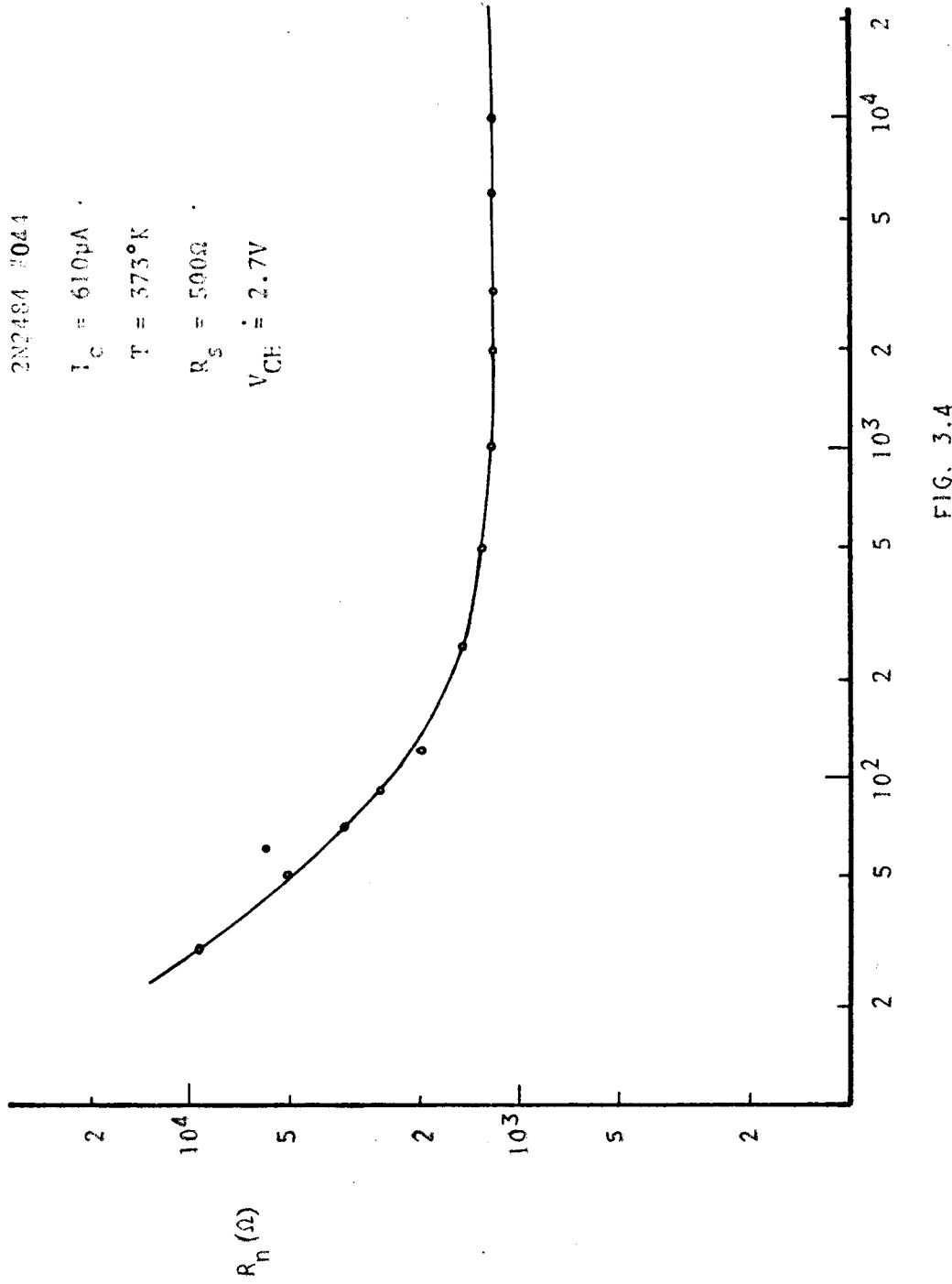


FIG. 3.4
 R_n as a function of frequency.

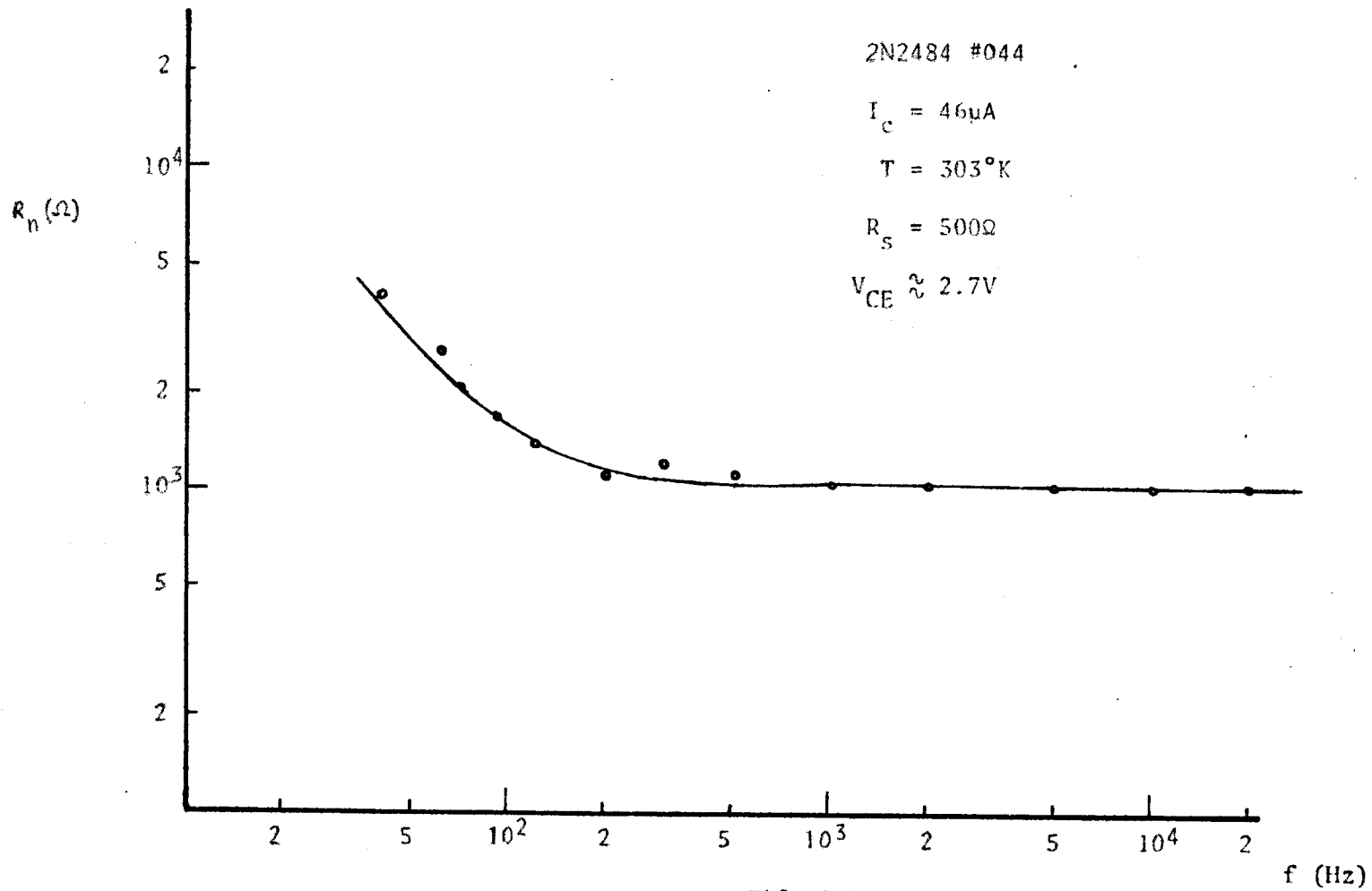
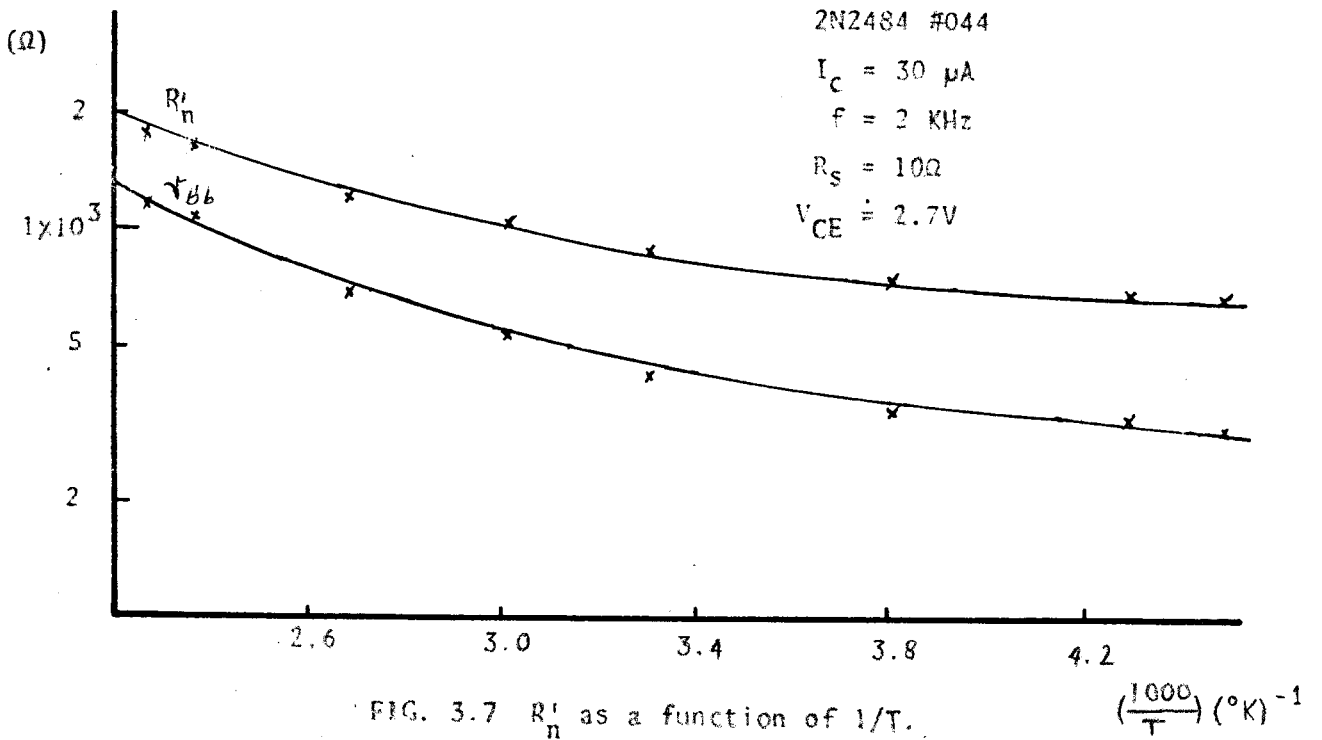
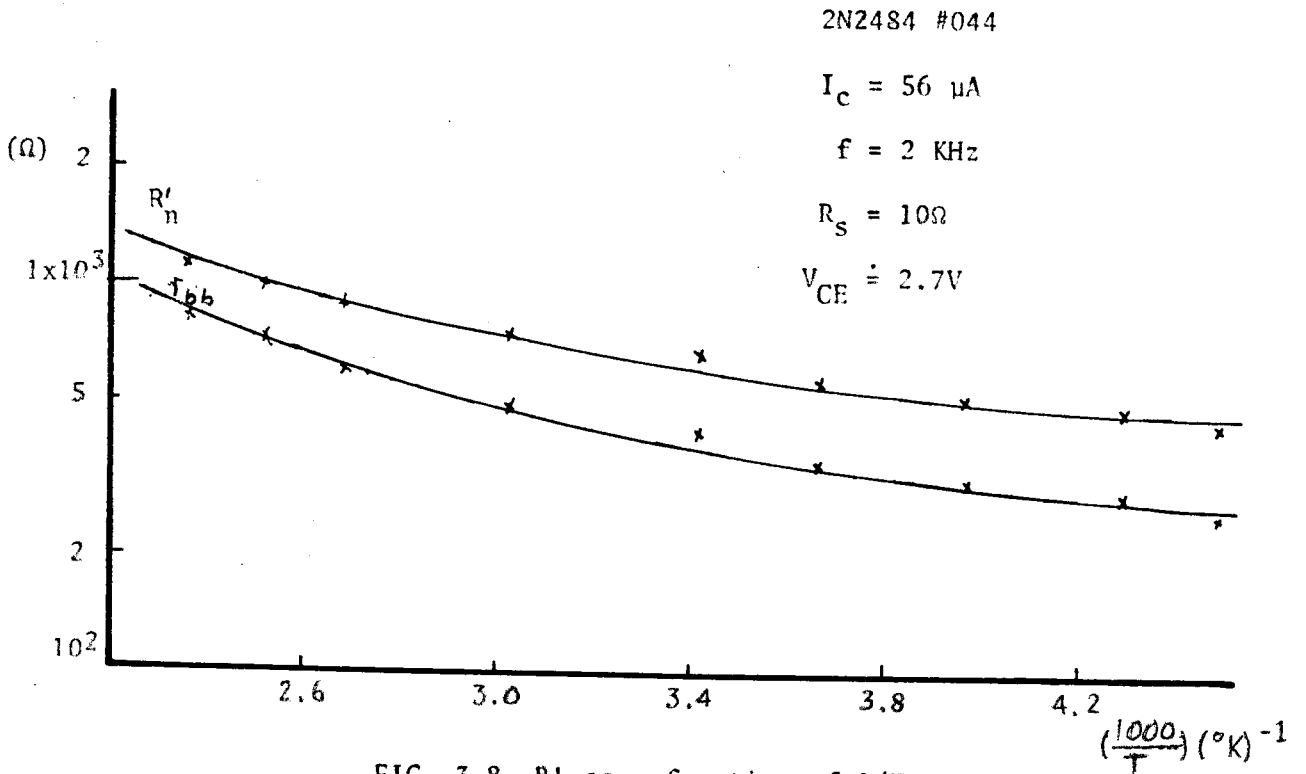
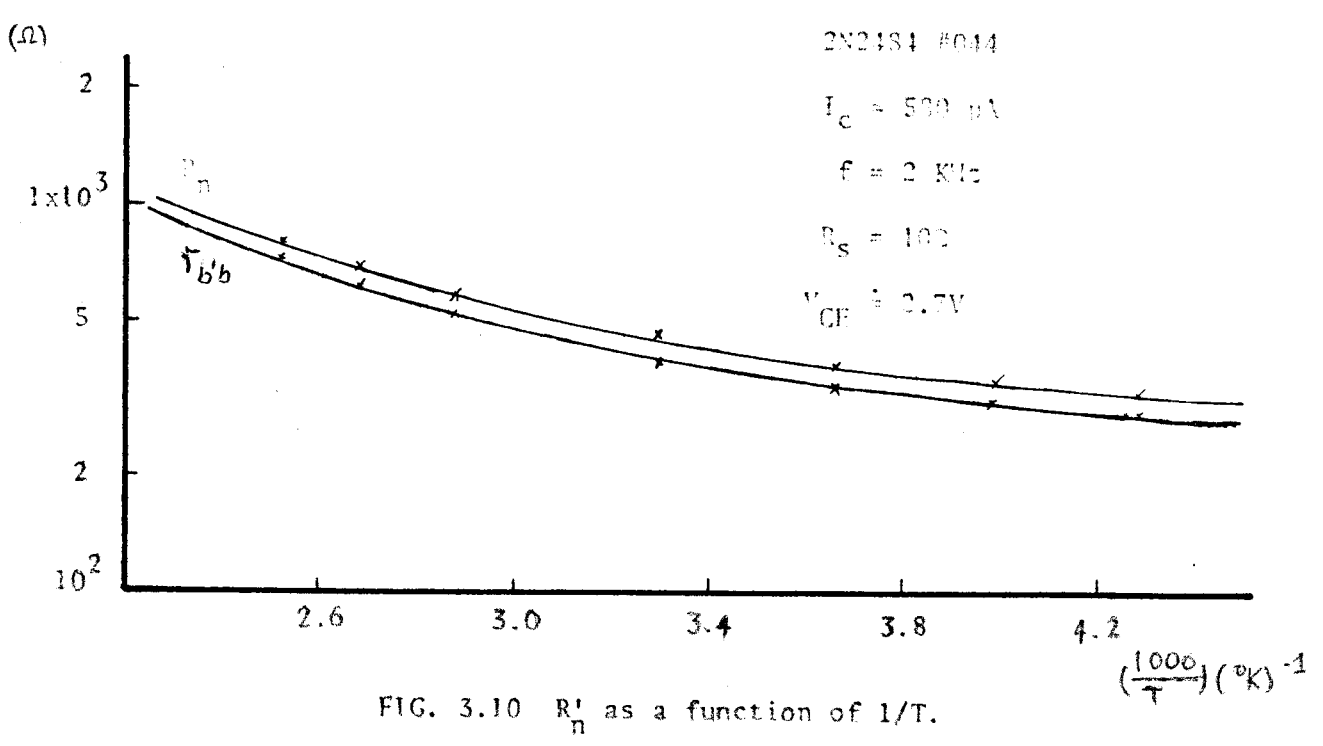
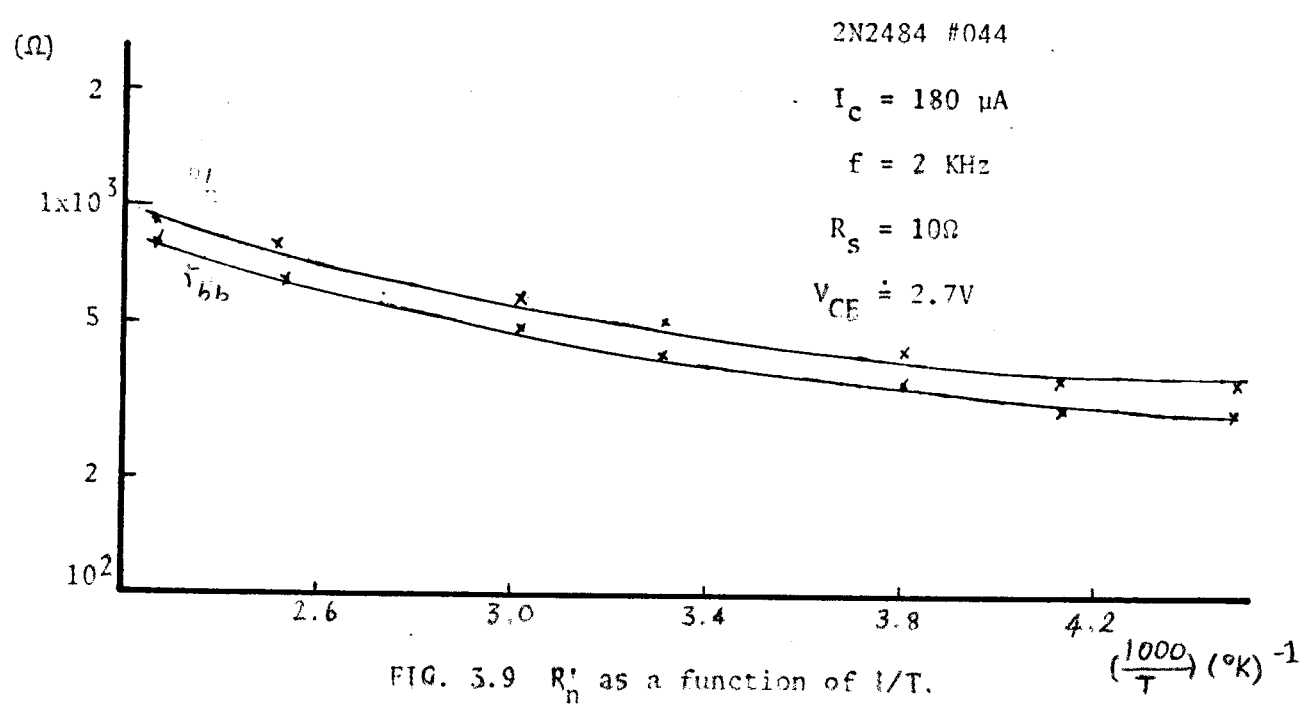
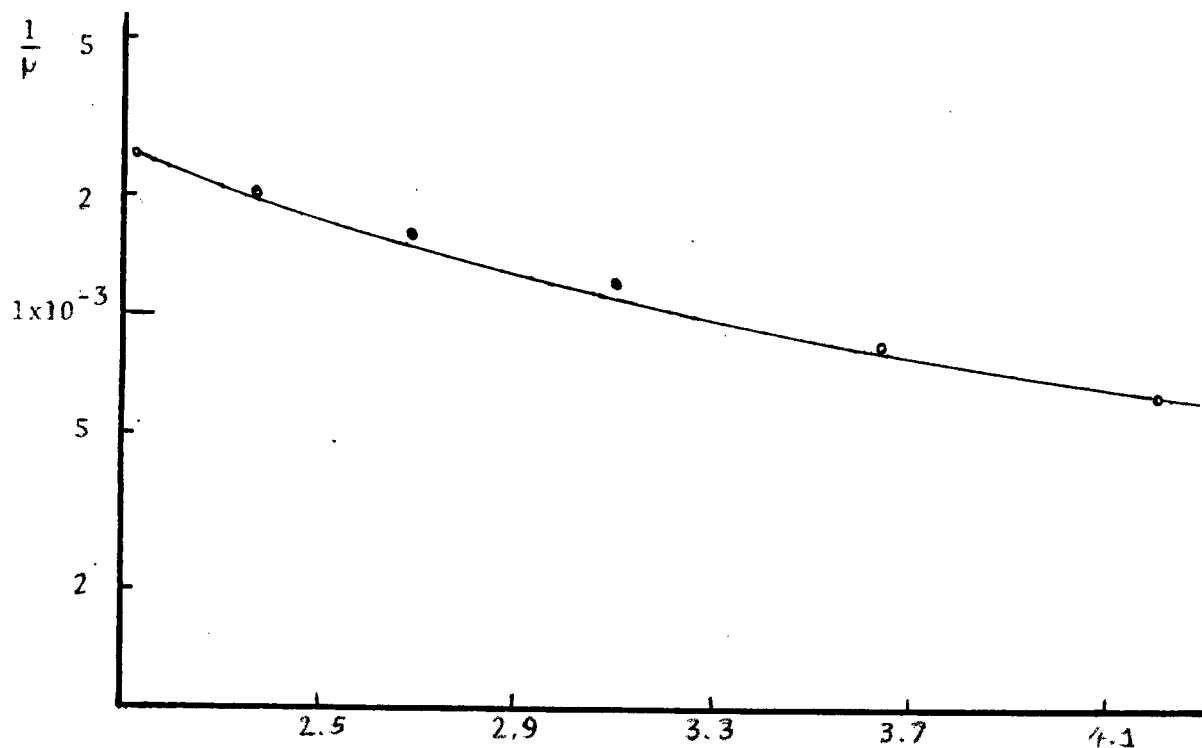


FIG. 3.6

R_n as a function of frequency.

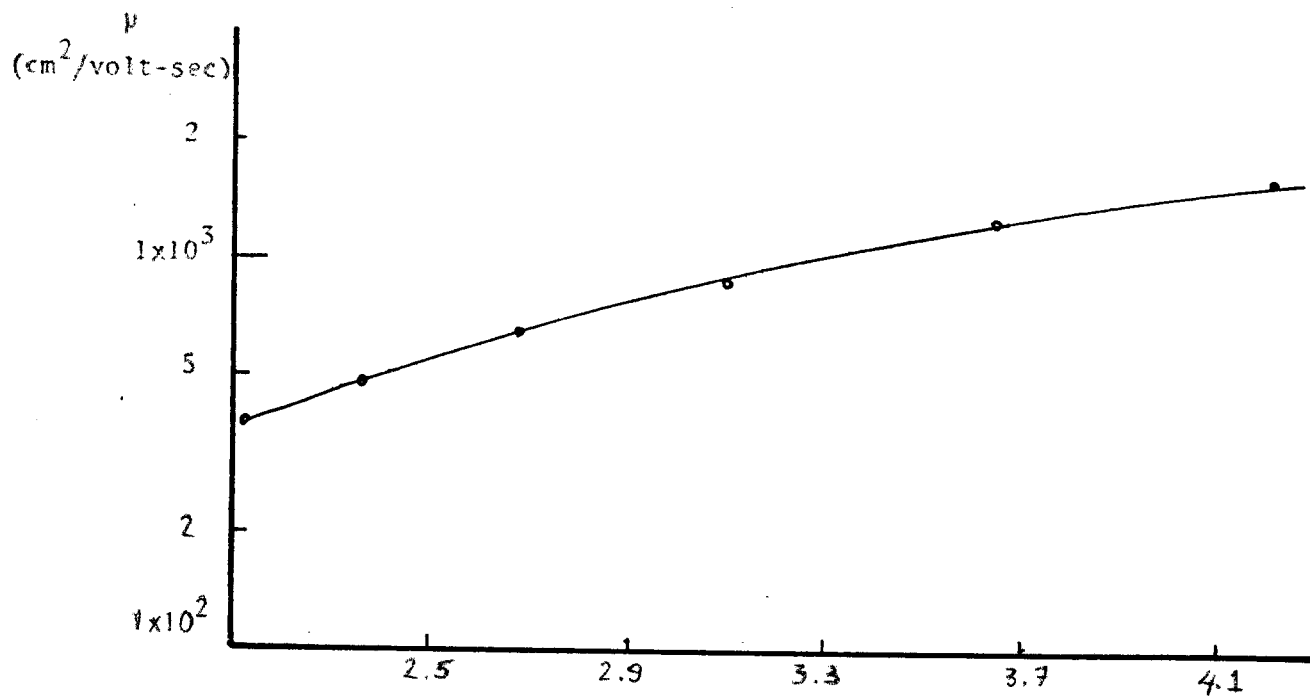






(b)
Resistivity as a function of $1/T$.

$\left(\frac{1000}{T}\right) (^{\circ}K)^{-1}$



(a)

$\left(\frac{1000}{T}\right) (^{\circ}K)$

FIG. 3.11 Electron mobility as a function of $1/T$.

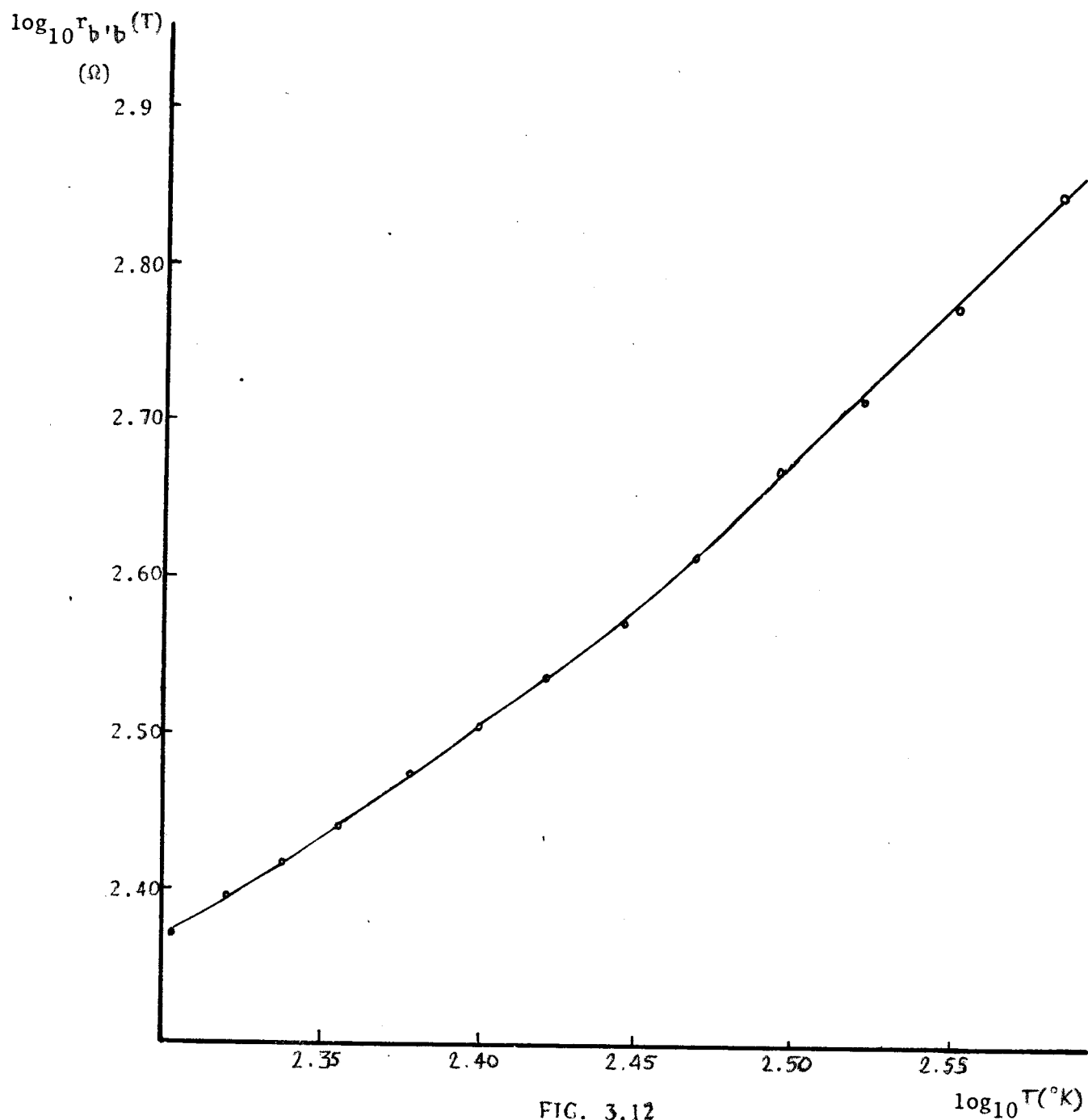


FIG. 3.12

$\log_{10} r_{b'b}(T)$ as a function of $\log_{10} T$.

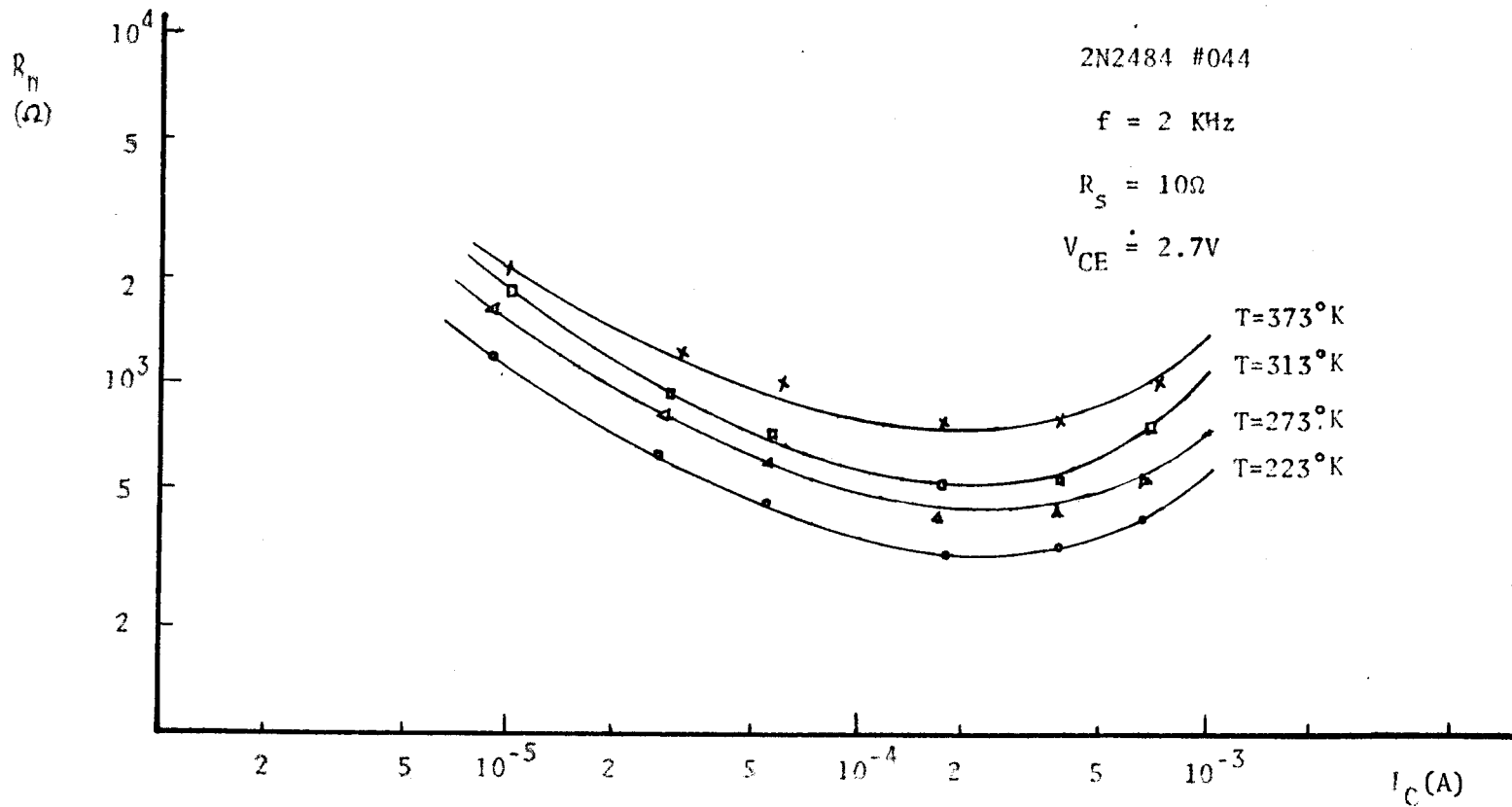


FIG. 3.13

R_{π} as a function of collector current with temperature as a parameter.

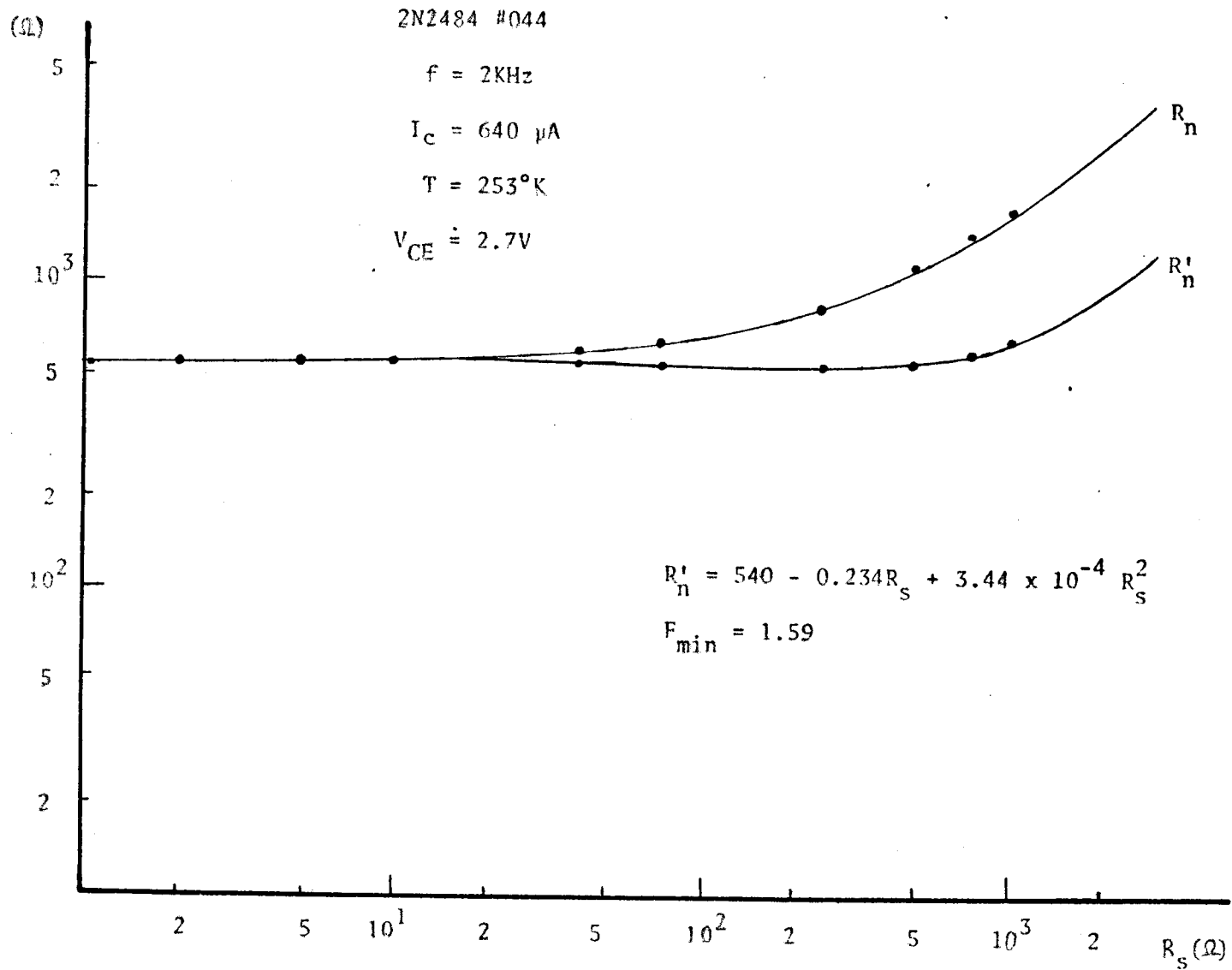


FIG. 3.14 R_n and R'_n as a function of R_s .

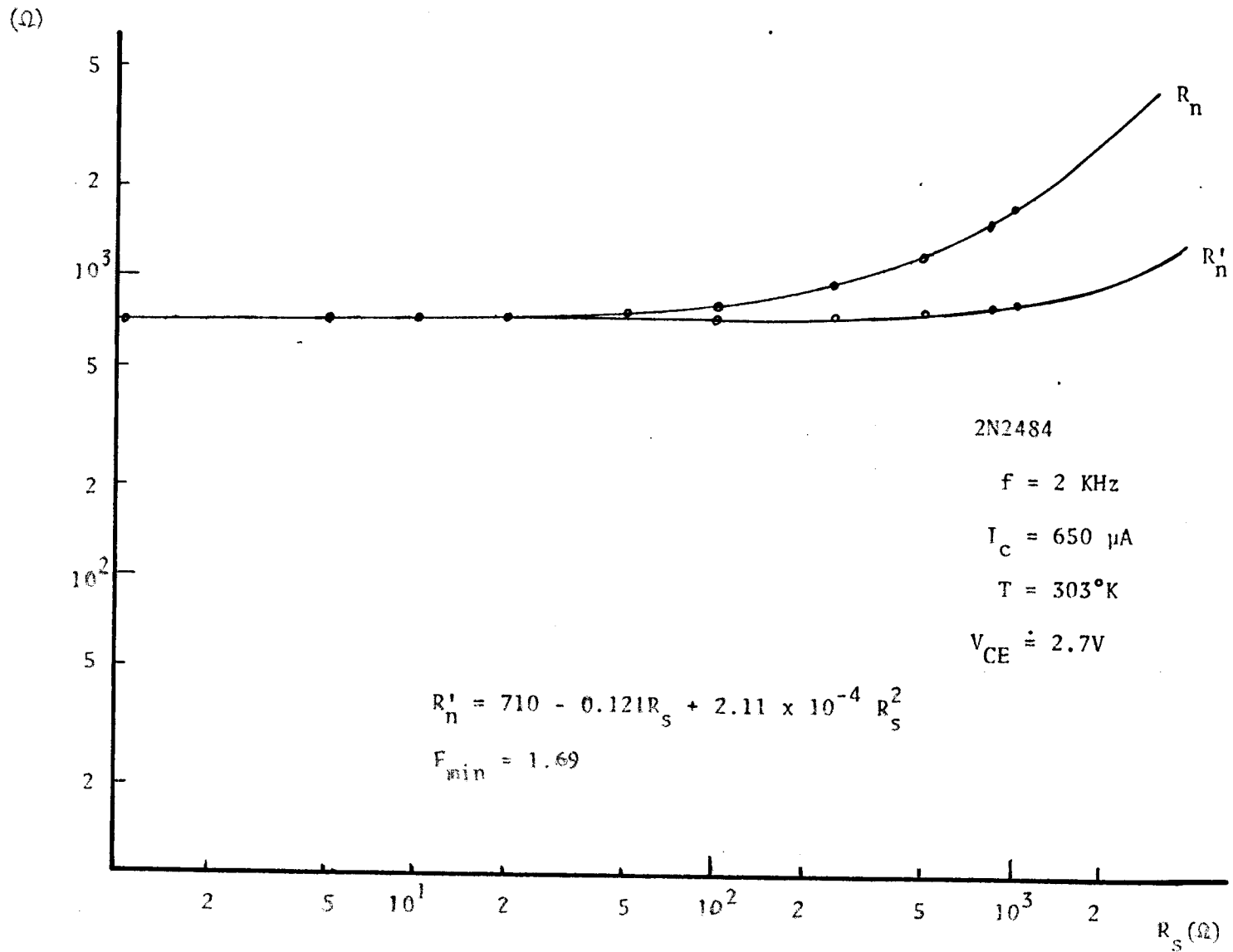


FIG. 3.15 R_n and R'_n as a function of R_s .

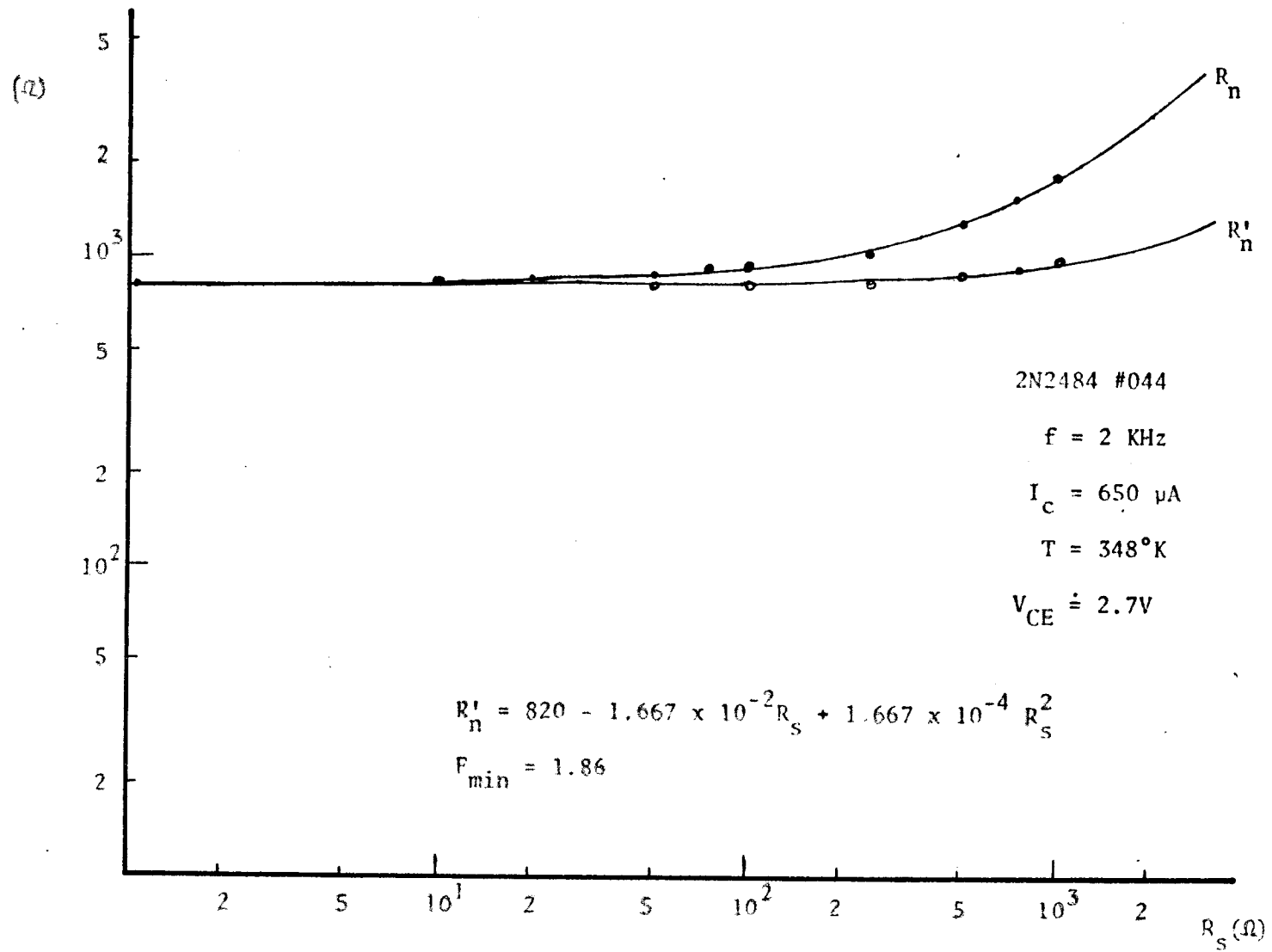


FIG. 3.16 R_n and R'_n as a function of R_S .

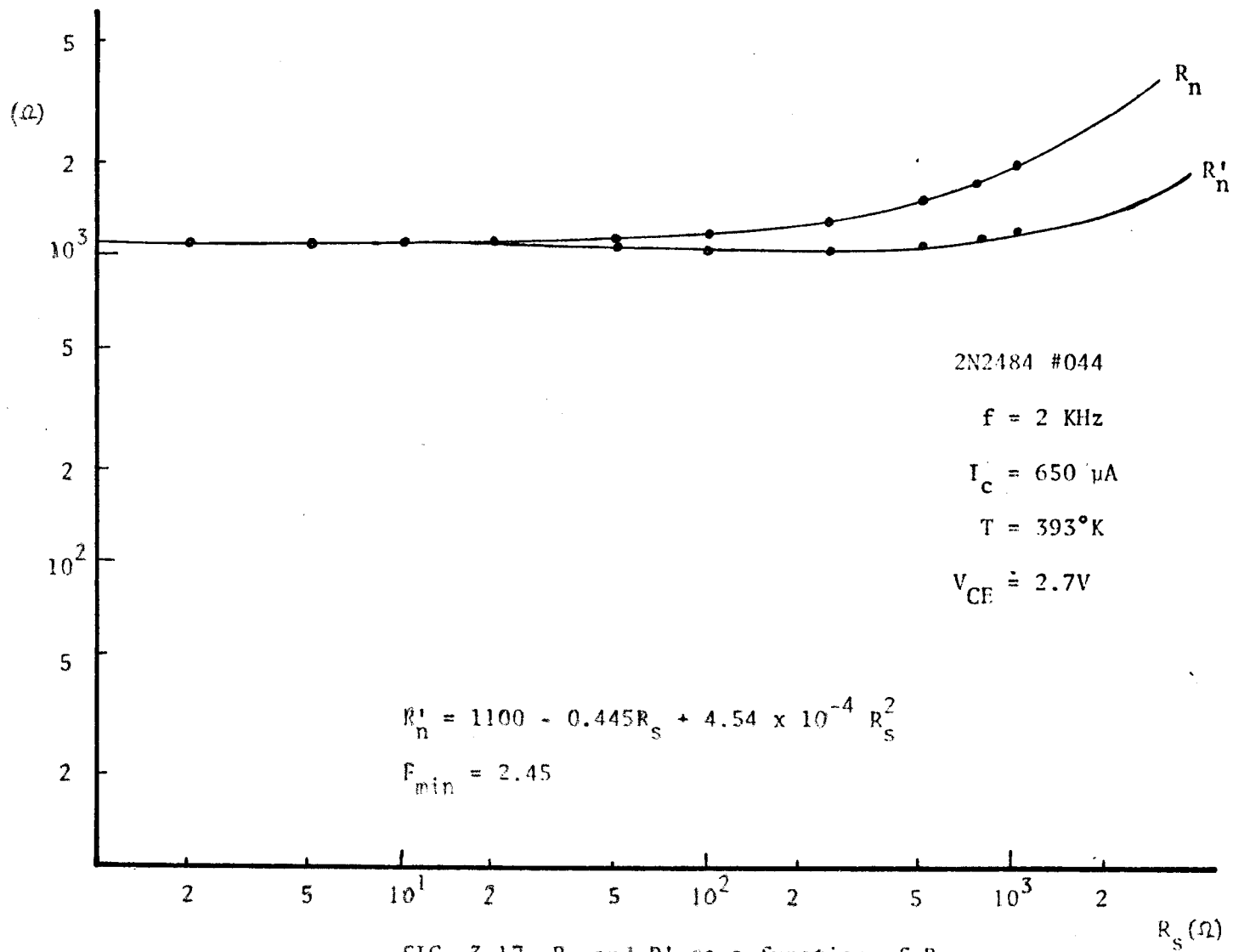


FIG. 3.17 R_n and R'_n as a function of R_s .

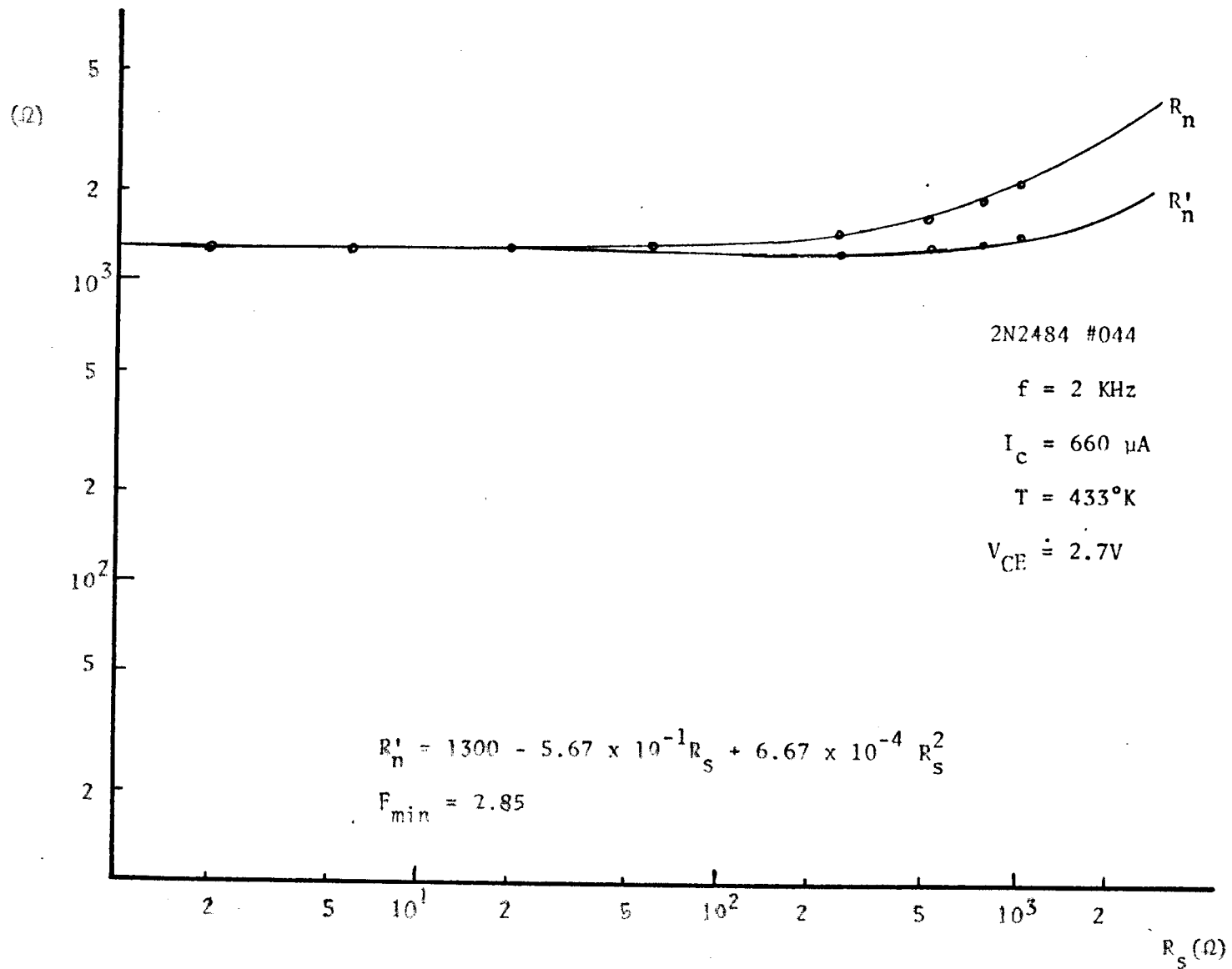


FIG. 3.18 R_n and R'_n as a function of R_s .

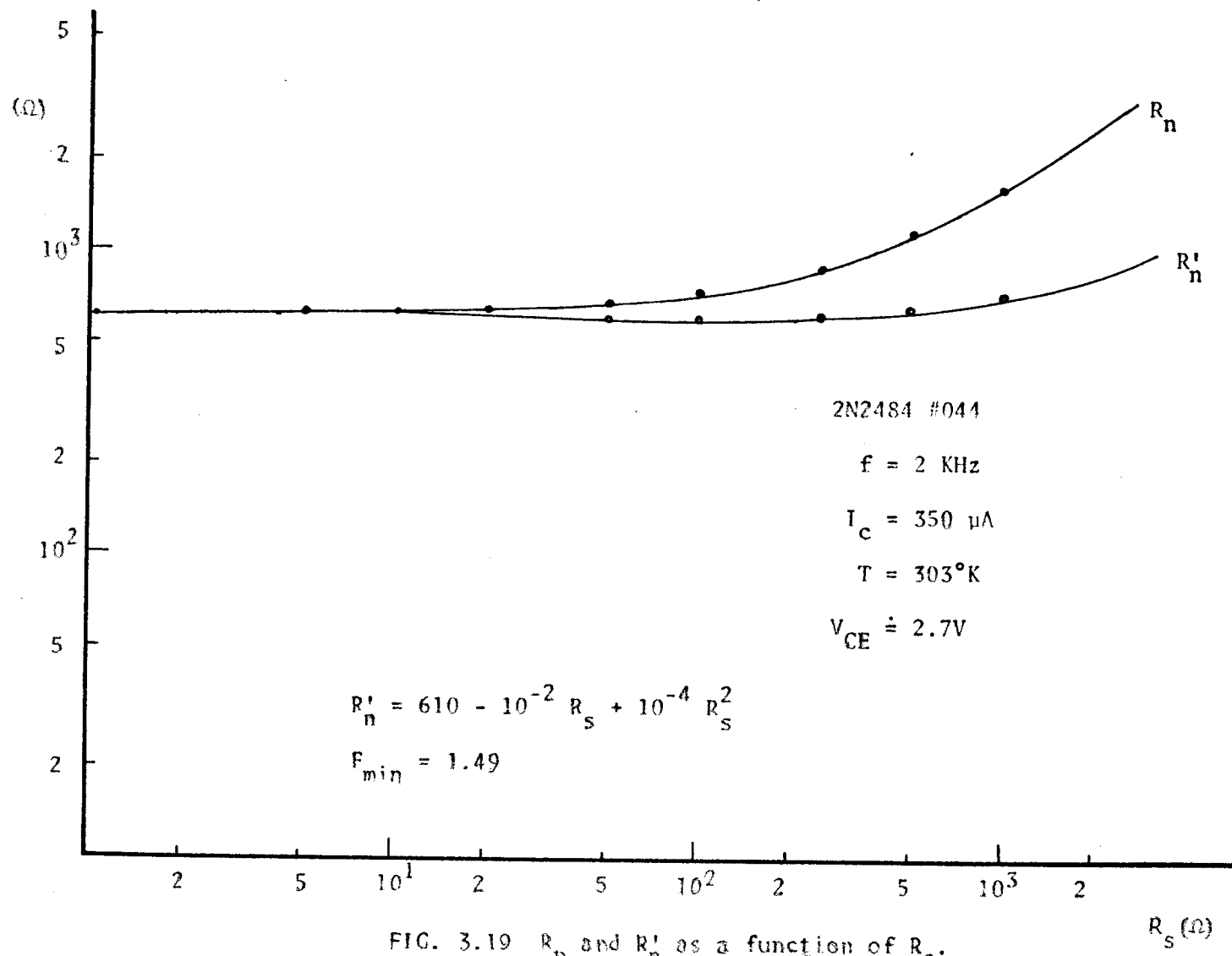


FIG. 3.19 R_n and R'_n as a function of R_s .

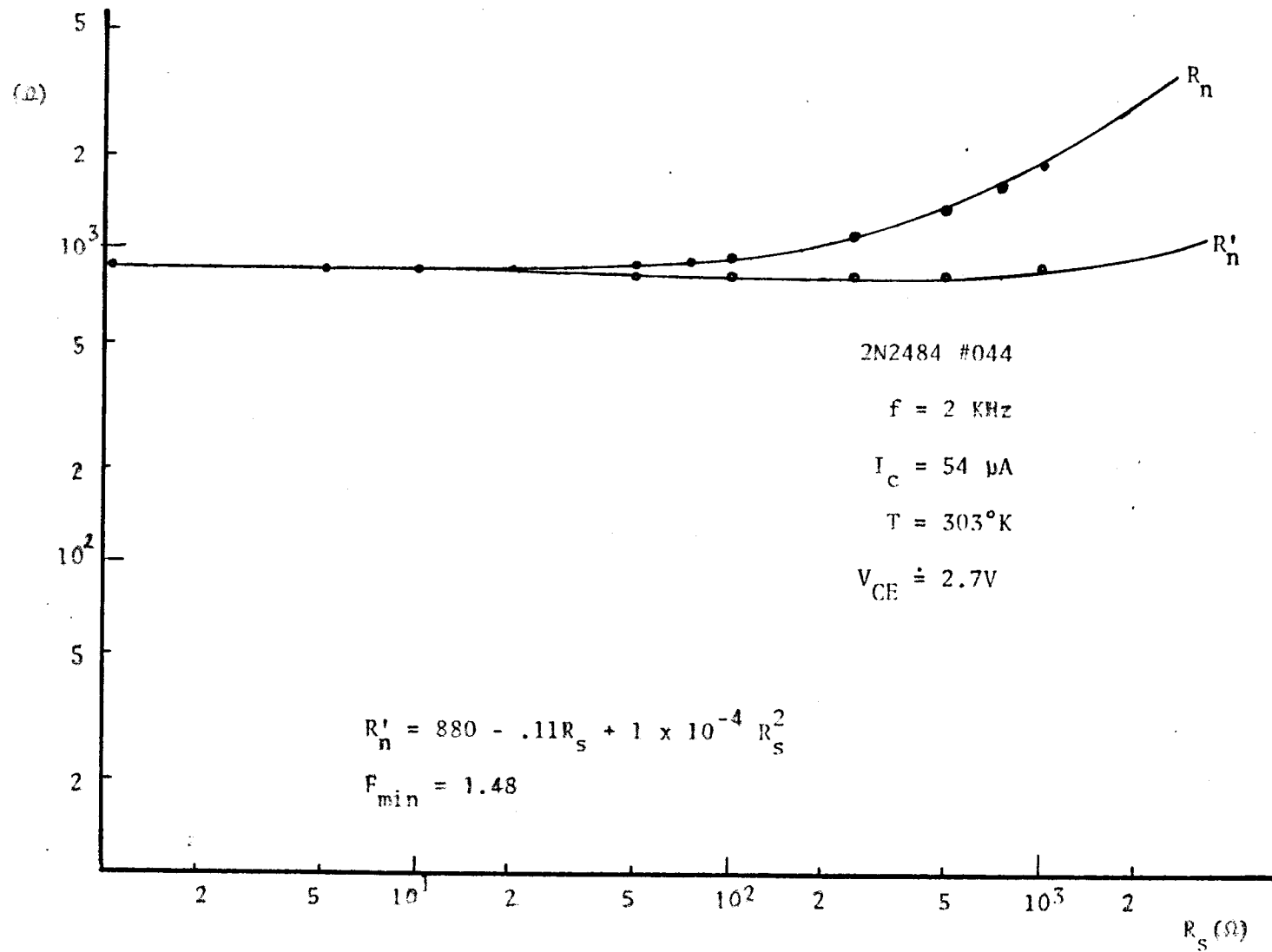


FIG. 3.20 R_n and R'_n as a function of R_S .

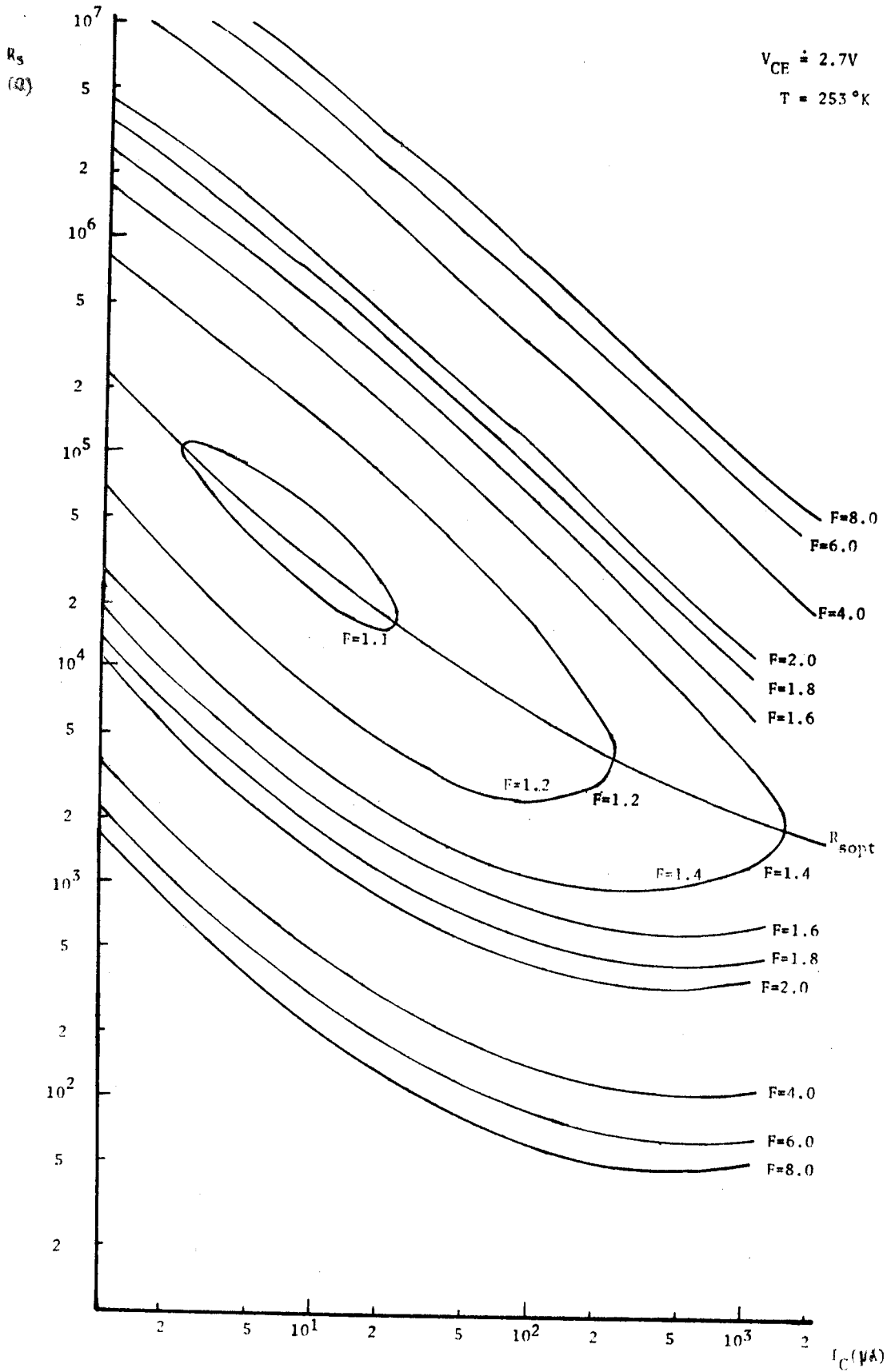


FIG. 3.21 Noise figure contours.

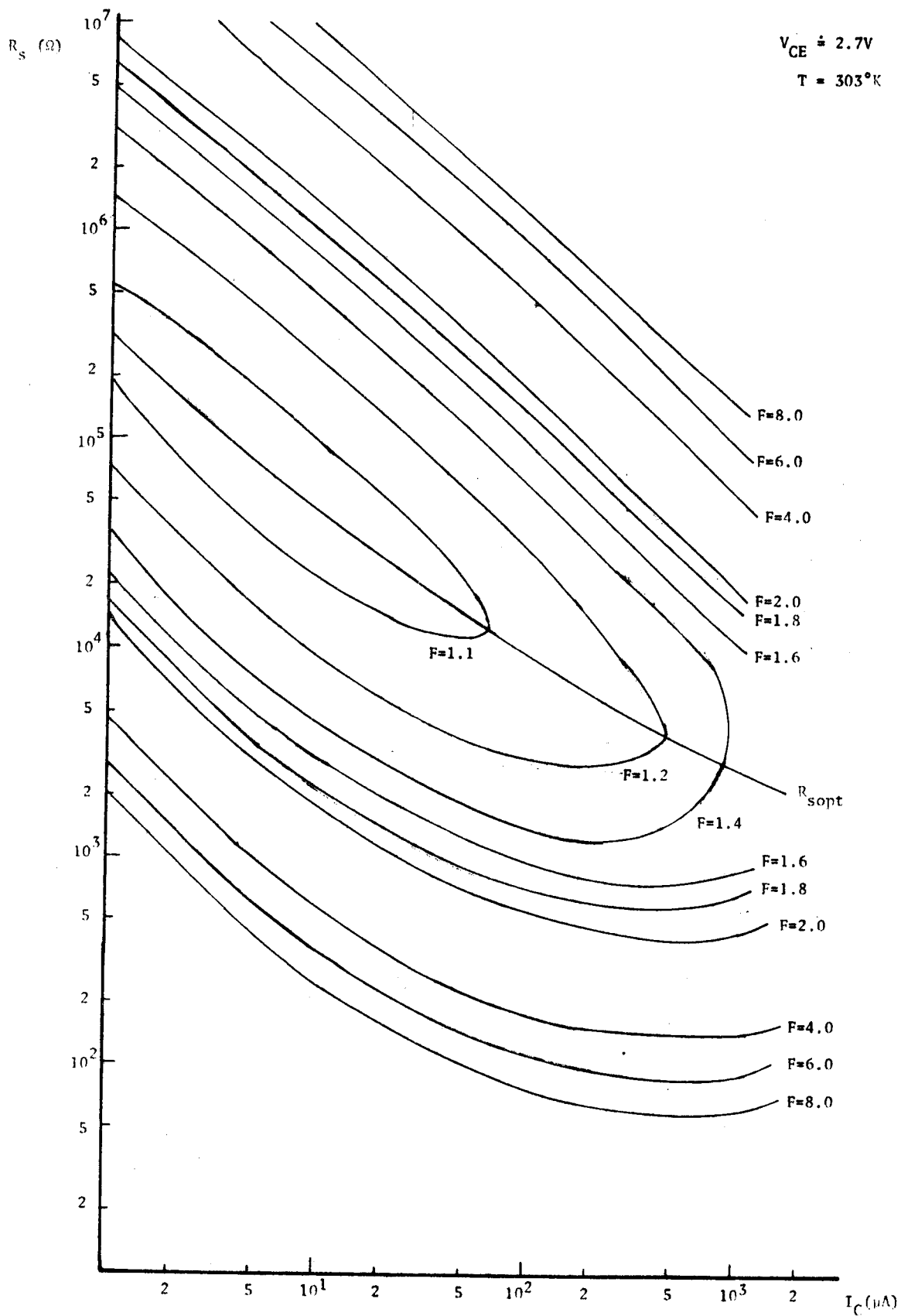


FIG. 3.22 Noise figure contours.

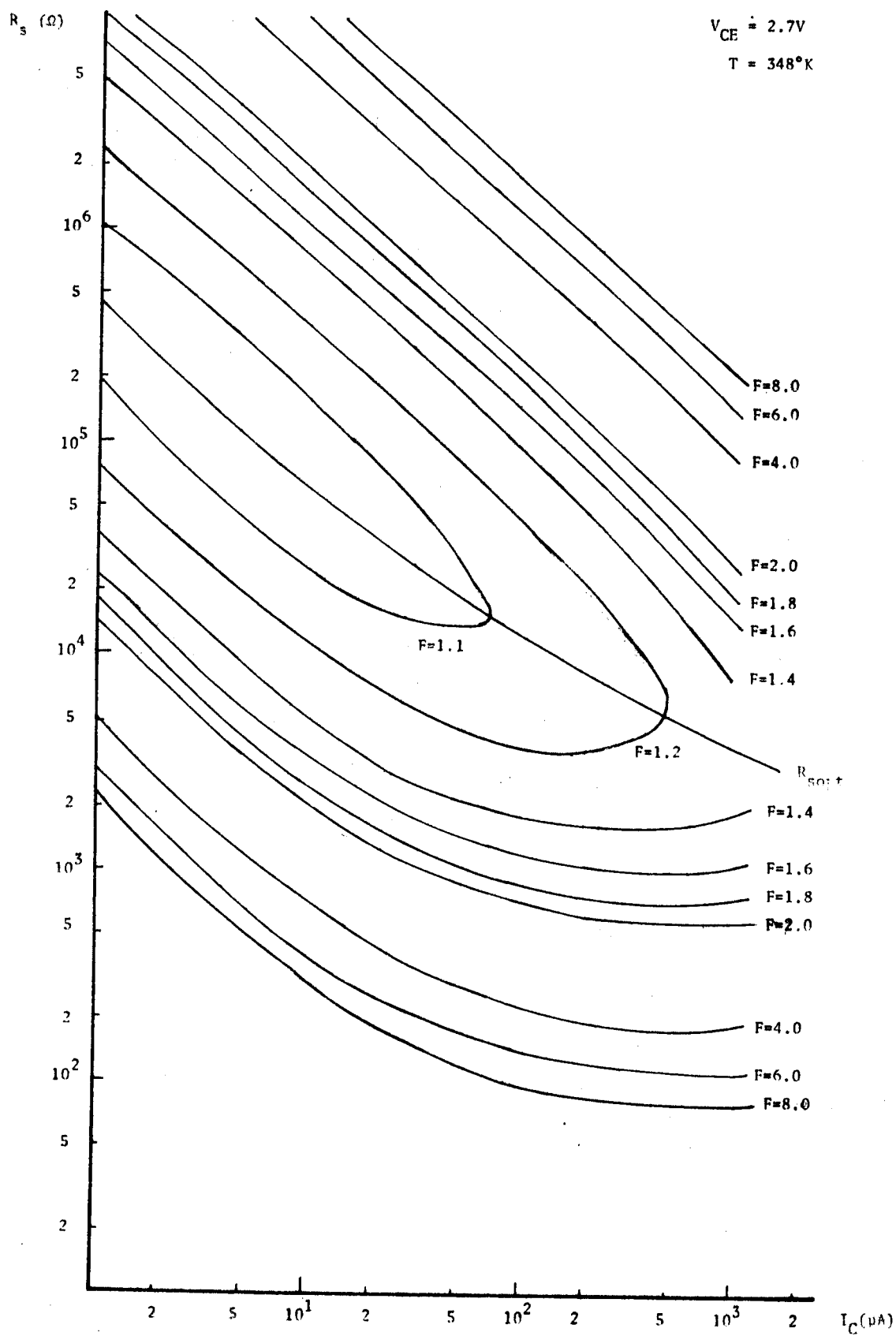


FIG. 3.23 Noise figure contours.

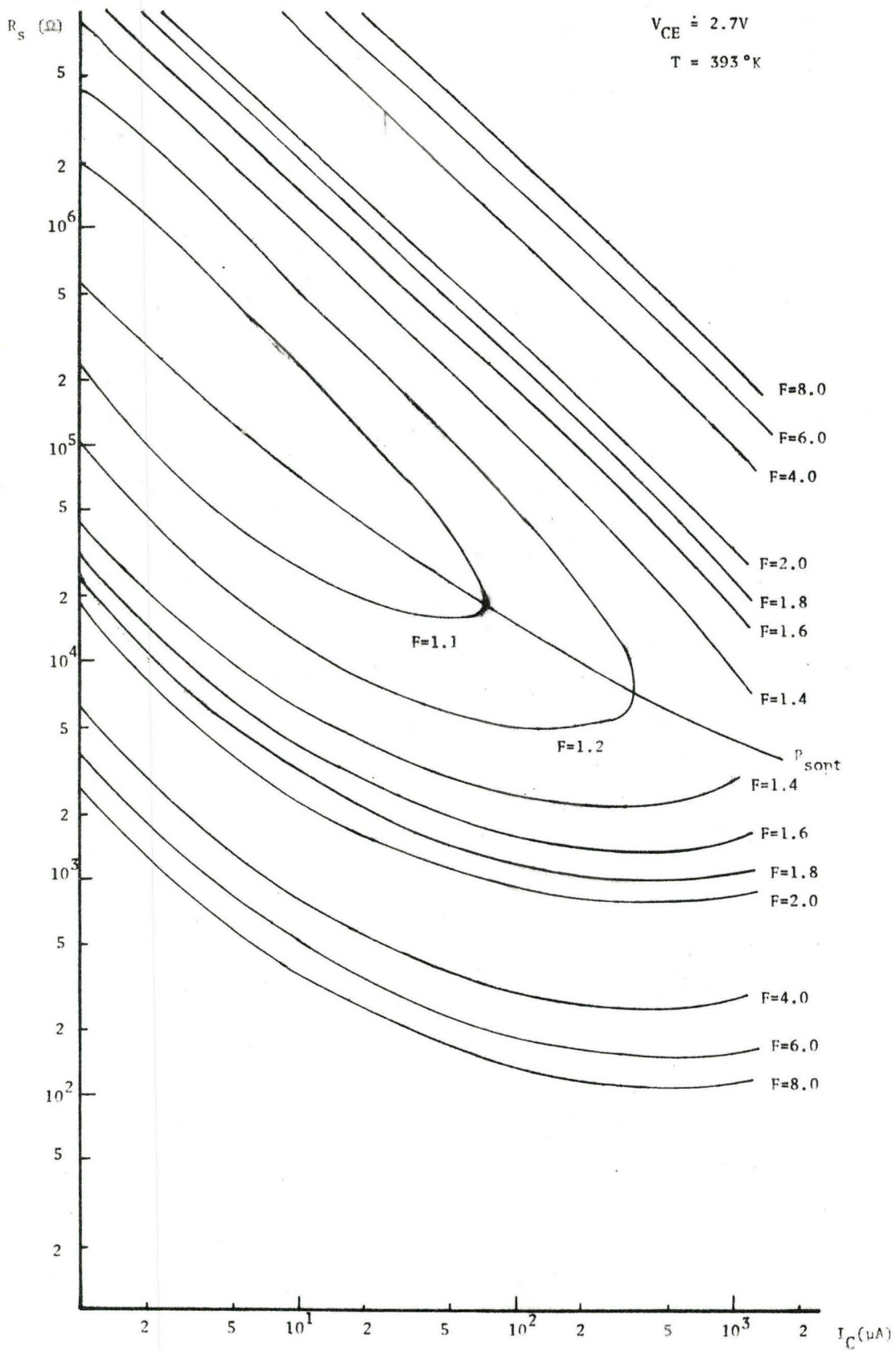


FIG. 3.24 Noise figure contours.

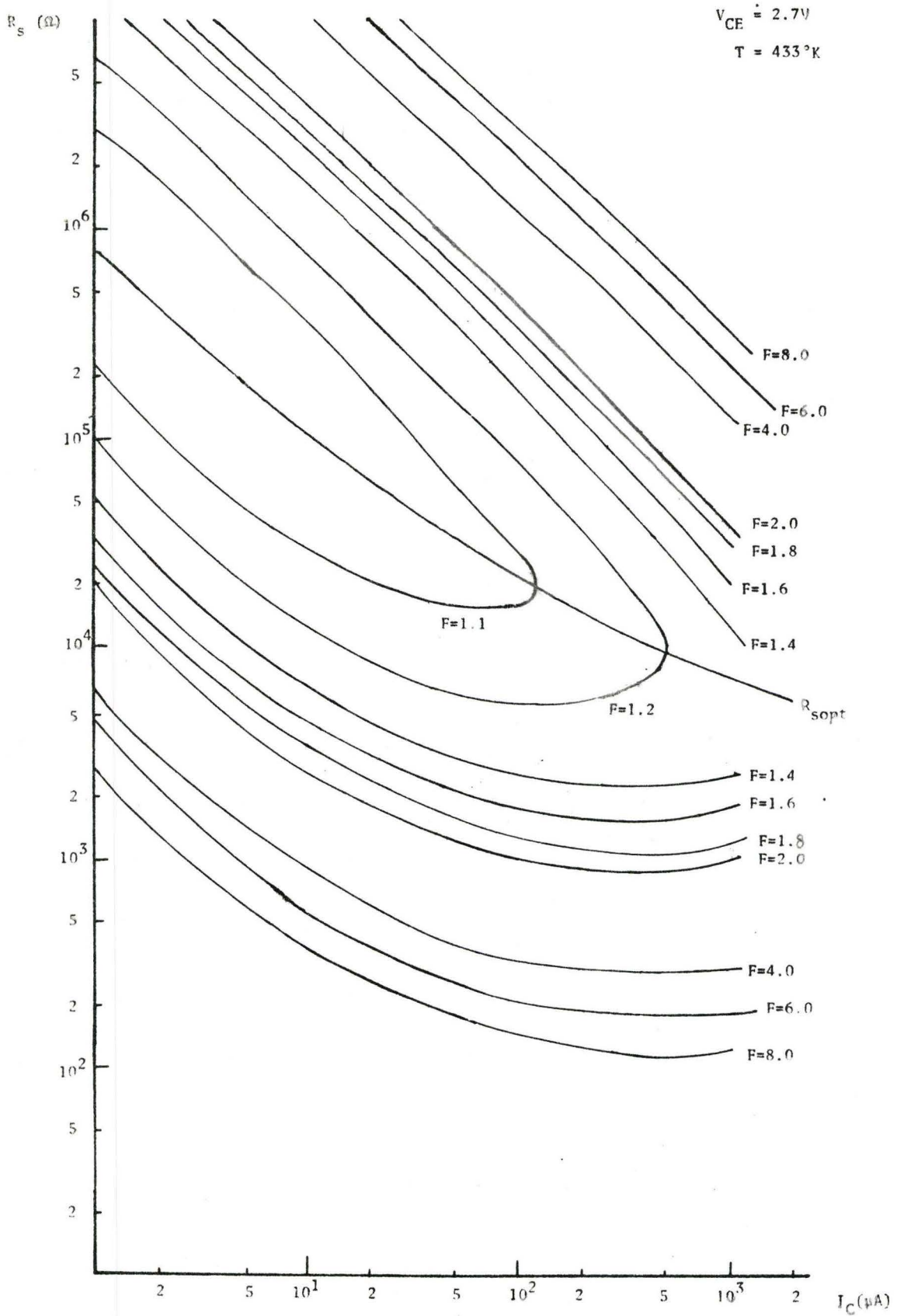


FIG. 3.25 Noise figure contours.

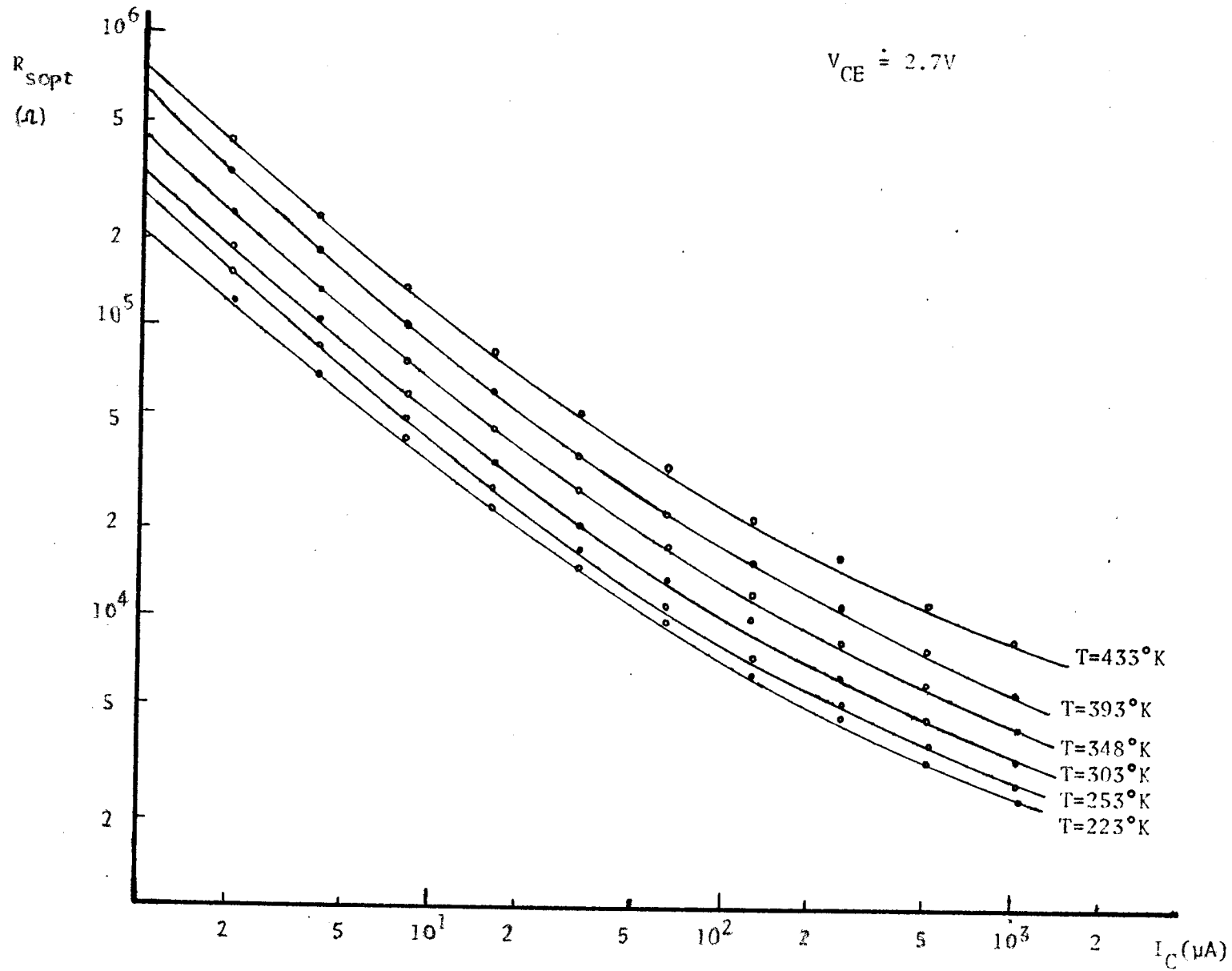


FIG. 3.26 Optimum source resistance as a function of I_C with temperature as a parameter.

CHAPTER 4

Conclusions

4.1 Synopsis

The main results of this investigation have been that the noise figure of a bipolar junction transistor is current and temperature dependent. In the investigation the base resistance of the device is found to be current independent but temperature dependent in the form $r_{b,b}(T) \propto T^{1.9}$. The resulting effect on this change in $r_{b,b}(T)$ is to degrade the noise performance of the BJT amplifier with temperature increment. However, this deterioration of the minimum noise figure over the temperature range of 303°K to 433°K is 2.28 db and 303°K to 253°K is -0.26 db. Thus, the lower the temperature the better the noise performance. However, operation of the device below 243°K is not recommended because the unpredictable nature of the burst noise limits the device performance. Also, the improvement in the noise performance of the device below room temperature is marginal.

The optimum source resistance value increases with temperature.

The 1/f noise region extends up to about 150 Hz. It is independent of temperature but a function of current flowing through the device.

At low frequency, up to 2 KHz, there is an additional noise source in the form of burst noise. Burst noise is a non-Gaussian noise and it is a function of the collector current and the ambient device temperature. The cyclic heating and cooling effect on the

device over the above temperature range was to reduce the pulse width and pulse rate of the burst noise.

The choice of a transistor for low noise amplification is based on several desirable characteristics:

1. the transistor be a low noise device.
2. the α -cutoff frequency of the transistor should be high enough so that the increase in noise near f_α does not degrade the average noise figure for the frequency range being used.
3. the current gain β_0 has to be sufficiently high to produce a high signal gain for the operating condition.

For given operating conditions of temperature and current, the optimum source resistance is chosen from the noise figure contours of Fig. 3.21-3.25 to yield F close to F_{opt} . F_{opt} obtained is independent of temperature.

The noise measurements demand considerable patience, nevertheless, the absolute accuracy cannot be expected to be better than 10 percent²⁴.

4.2 Suggestions for Further Work

The "thermal cycling" effect on the burst noise of a device should be more thoroughly studied and characterized.

The analogous behaviour of mobility and base resistance with respect to temperature suggests that the mobility behaviour at extreme temperatures would be reflected in the base resistance behaviour and

noise performance. Any deviation from this would suggest additional sources of noise. This hypothesis should be investigated at extreme temperatures, especially at liquid nitrogen temperature.

This work could be extended to higher frequency transistors.

REFERENCES

1. Gupta, M.S., "Noise in avalanche transit-time devices", Proc. IEEE, vol. 59, No. 12, pp. 1674-1687, Dec. 1971.
2. Roig, G.A., "Transistor noise at extreme temperatures", Ph.D. Thesis, University of Florida, Dec. 1970.
3. Hanson, G.H. and van der Ziel, A., "Shot noise in transistors", Proc. IRE, vol. 45, pp. 1538-1542, 1957.
4. Gibbons, J.F., "Low frequency noise and its application to the measurements of certain transistor parameters", Trans. IRE, ED. 9, pp. 308-315, May 1962.
5. Plumb, J.L. and Chenette, E.R., "Flicker noise in transistors", IEEE Trans., ED. 10, pp. 304-308, Sept. 1963.
6. van der Ziel, A. and Tong, H., "Low-frequency noise predicts when a transistor will fail", Electronics, pp. 95-97, Nov. 28, 1966.
7. Rheinfelder, W.A., "Design of low-noise transistor input circuits", Hayden Book Co., N.Y., 1964.
8. van der Ziel, A., "Fluctuation phenomena in semiconductors", Butterworths Sci. Pub., London, 1959.
9. Jaeger, R.C. and Brodersen, A.J., "Low frequency noise sources in BJTS", IRE Trans. Electron Devices, vol. ED-17, No. 2, pp. 128-136, Feb. 1970.
10. Hsu, S.T., "Bistable noise in p-n junctions", Solid State Electronics, vol. 14, pp. 487-497, 1971.

11. Hsu, S.T. and Whittier, R.J., "Characterization of burst noise in silicon devices", Solid State Electronics, vol. 12, pp. 867-878, 1969.
12. Gray, P.E., Dewitt, D., Boothroyd, A.R. and Gibbons, J.F., "Physical electronics and circuit models for transistors", SEEC, vol. 3, Chapter 3, Wiley, 1964.
13. van der Ziel, A., "Theory of shot noise in junction diode and junction transistors", Proc. IRE, vol. 43, pp. 1639-1646, 1955.
14. ———, "Noise in solid state devices and lasers", Proc. IEEE, vol. 58, No. 8, pp. 1178-1206, Aug. 1970.
15. Chenette, E.R., "Noise in semiconductor devices", Adv. in Electronics and Electron Physics, vol. 23, Academic Press, Inc., N.Y., 1967.
16. Schneider, B. and Strutt, M.J.O., "Theory and experiment on shot noise in silicon p-n junctions and transistors", Proc. IRE, vol. 47, pp. 546-554, April 1959.
17. Nielsen, E.G., "Behaviour of noise figure in junction transistors", IRE, vol. 45, pp. 957-963, July 1957.
18. Faulkner, E.A., "Optimum design of low noise amplifiers", Electronics Letters, vol. 2, no. 11, pp. 426-427, 1967.
19. Pierce, J.F., "Transistor circuit theory and design", Merrill Books, 1963.
20. Chenette, E.R. and van der Ziel, A., "Accurate noise measurements of transistors", IRE Trans. ED, pp. 123-128, March 1962.
21. Martin, J.C., Esleve, D., deCacquery, A and Ribenyrol, J.M., " $1/f$ noise in silicon planar transistors", Proc. Nottingham Conf. on

physical aspects of Noise, Sept. 1968.

22. Luque, A. Mulet, J., Rodriguez, R. and Segovia, R., "Proposed dislocation theory of burst noise in planar transistors", Electronics Letters, vol. 6, No. 8, pp. 176-178, March 19, 1970.
23. Sze, S.M., "Physics of semiconductor devices", Chapter 1.5, Wiley, N.Y., 1969.
24. Klassen, F.M. and Robinson, J.R., "Anomalous noise behaviour of the JGFET at low temperatures", IEEE Trans. Electron Devices, vol. ED-17, No. 10, pp. 852-857, Oct. 1970.
25. Hsu, S.T., "Noise in high gain transistors and its application to the measurement of certain transistor parameters", IEEE Trans. Electron Devices, vol. ED-18, No. 7, pp. 425-431, July 1971.
26. Malaviya, S.D., "Study of noise in transistor at microwave frequencies up to 4 GHz", Ph.D. Thesis, University of Minnesota, 1969.

Appendix A

Amplifiers in Parallel

18

Faulkner has developed a technique which has been used by him to improve the noise figure of audio-frequency amplifying systems where the source impedance is $1\text{ K}\Omega$ or less.

The design is based on the fact that when n identical amplifiers are connected in parallel, the series noise resistance, $r_{b'b} + \frac{1}{2} r_e$, and parallel noise resistance, $2\beta_o r_e$, are both reduced by a factor n compared with the corresponding value for one of the amplifiers.

The parallel setup of the transistors is shown in Fig. A.1.

Proof: Consider the signal/noise ratio given by the parallel combination for very low and very high source impedances. When $R_s \rightarrow 0$, the mean square signal current delivered into the load is increased by a factor n^2 compared with a single amplifier, but the mean square noise current is only increased by a factor n , because the noise generators of the individual amplifiers are not correlated; thus the signal/noise ratio is improved by a factor n compared to that given by a single amplifier.

When $R_s \rightarrow \infty$, the source current is shared between the amplifiers, and the signal-output current is only the same as that available from a single amplifier; so the total signal/noise ratio is deteriorated by a factor n .

Comparing the result with equation (2.54) shows that both $r_{b'b} + \frac{1}{2} r_e$ and $2\beta_o r_e$ have been reduced by a factor n , owing to the parallel connection of the transistors.

An extension of this argument shows that, if the n amplifiers have different values of the base resistance, the appropriate formula for the series noise resistance of the combination is $n^{-2} \sum (r_{b'b} + \frac{r_e}{2})$.

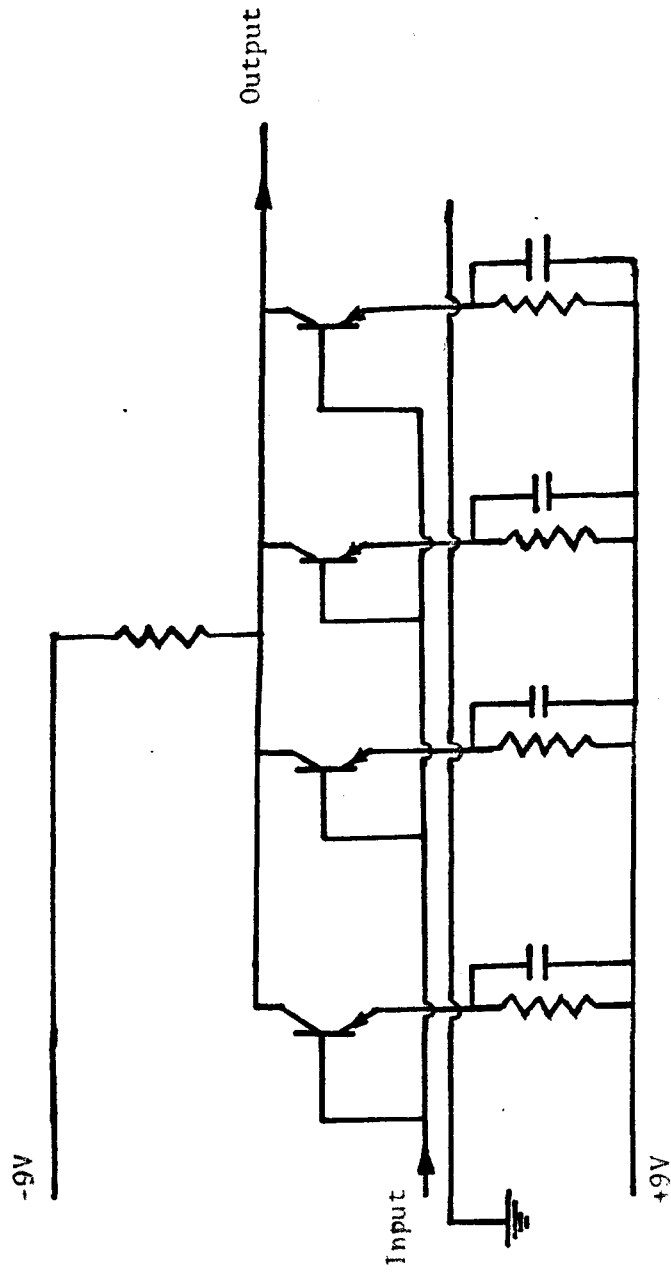


FIG. A.1

Amplifiers in parallel for low noise input circuit.

Appendix B

To Show That Noise Contribution is Only Due to the TUT

Each of the transistors in Fig. 3.2 is replaced by a noise free transistor and noise generators of the device, as shown in Fig. B.2. A hybrid- Π model is used here to show that assumptions of one model are equally valid for another.

From Fig. B.1,

$$V_0 = -g_{m2} R_L \cdot V_2 \quad (\text{B.1})$$

$$V_1 = \frac{r_{\pi 1}}{r_{\pi 1} + r_{b'b} + R_s} V_s \quad (\text{B.2})$$

At node E_2 ,

$$g_{m2} V_2 = g_{m1} V_1 - g_{\pi 2} V_2 \quad (\text{B.3})$$

$$\frac{V_2}{V_1} = \frac{g_{m1}}{g_{m2} + g_{\pi 2}} \quad (\text{B.4})$$

For voltage across $C_1 E_1$

$$\begin{aligned} V' &= -V_2 + (-g_{\pi 2} V_2) r_{b'b} \\ &= -V_2 [1 + g_{\pi 2} r_{b'b}] \end{aligned} \quad (\text{B.5})$$

But $g_{\pi 2} r_{b'b} \ll 1$

$$\therefore V' = -V_2 \quad (\text{B.6})$$

From equations (B.1) and (B.5)

$$\frac{V_0}{V_1} = \frac{-g_{m2}R_L}{1 + g_{\pi 2}r_{b'b}} \quad (\text{B.7})$$

Overall voltage gain

$$\begin{aligned} \frac{V_0}{V_s} &= -g_{m2}R_L \cdot \frac{g_{m1}}{g_{m1} + g_{\pi 2}} \cdot \frac{r_{\pi 1}}{r_{\pi 1} + r_{b'b} + R_s} \\ &\doteq -g_{m2}R_L \cdot \frac{r_{\pi 1}}{r_{\pi 1} + R_s} \end{aligned} \quad (\text{B.8})$$

and

$$\begin{aligned} \frac{V_1}{V_s} &= \frac{V_0}{V_s} \cdot \frac{V_1}{V_0} = \frac{V_0}{V_s} \cdot \frac{V_1}{V_2} \cdot \frac{V_2}{V_0} \\ &= -g_{m2}R_L \cdot \frac{g_{m1}}{g_{m1} + g_{\pi 2}} \cdot \frac{r_{\pi 1}}{r_{\pi 1} + r_{b'b} + R_s} \cdot -[1 + g_{m1}r_{b'b}] \cdot \frac{-1}{g_{m2}R_L} \end{aligned} \quad (\text{B.9})$$

From Fig. (B.2).

Noise output due to $V_{nb'b1}$ is obtained from equation (B.8)

$$\overline{V_{0b'b}^2} = \left[g_{m2}R_L \cdot \frac{g_{m1}}{g_{m1} + g_{\pi 2}} \cdot \frac{r_{\pi 1}}{r_{\pi 1} + r_{b'b} + R_s} \right]^2 \cdot \overline{V_{nb'b1}^2} \quad (\text{B.10})$$

short circuit output current

$$\overline{i_{0b'b1}^2} = [g_{m1} V_2]^2 \quad (\text{B.11})$$

Substituting for V_2 from equations (B.4) and (B.2)

$$\overline{i_{0b'b1}^2} = \left[g_{m1} \cdot \frac{g_{m1}}{g_{m1} + g_{\pi 2}} \cdot \frac{r_{\pi 1}}{r_{\pi 1} + r_{b'b} + R_s} \right]^2 \overline{V_{nb'b1}^2} \quad (\text{B.12})$$

$$r_{\pi} \gg r_{b'b} + R_s$$

$$g_m r_{\pi} = \beta_0$$

$$\therefore \overline{i_{0b'b1}^2} \doteq \left[\frac{\beta_0}{r_{\pi} + r_{b'b} + R_s} \right]^2 \cdot \overline{V_{nb'b1}^2} \quad (\text{B.13})$$

Noise output due to $V_{nb'b2}$

From Fig. B.3

$$g_{\mu} \doteq \eta g_{\pi}$$

$$g_0 \doteq \eta g_{\mu} \quad (\text{B.14})$$

where

$$\eta = \frac{1}{\beta_0}$$

The output current

$$\begin{aligned} i_0 &= g_m V - g_{\mu} V_B \\ &= g_m (V_B - V_E) - g_{\mu} V_B \end{aligned} \quad (\text{B.15})$$

At node E

$$(g_m + g_{\pi}) V = V_E \cdot \eta g_m \quad (\text{B.16})$$

At node B

$$\begin{aligned} g_{b'b} (\overline{V_{nb'b2}} - V_B) &= g_{\pi} V + g_{\mu} V_B \\ g_m \overline{V_{nb'b2}} &= V_B [g_{b'b} + g_{\pi} + g_{\mu}] - g_{\pi} V_E \end{aligned} \quad (\text{B.17})$$

From equation (B.16)

$$(g_m + g_{\pi}) (V_B - V_E) = V_E \cdot \eta g_m \quad (\text{B.18})$$

$$V_E = \frac{g_m + g_\pi}{ng_m + g_m + g_\pi} \cdot V_B$$

Hence, equation (B.17) becomes

$$g_{b'b} V_{nb'b2} = V_B \{ [g_{b'b} + g_\pi + g_\mu] - g_\pi \cdot \frac{(g_m + g_\pi)}{g_m + g_\pi + ng_m} \} \quad (B.19)$$

Simplifying equation (B.15) using equations (B.16) - (B.19)

$$i_0 \doteq [ng_m - g_\mu] \cdot V_{nb'b2} \quad (B.20)$$

$$\therefore \overline{i_{0b'b2}^2} = (ng_m)^2 \overline{V_{nb'b2}^2} \ll g_m^2 \overline{V_{nb'b1}^2}$$

Hence, the noise power at the output is due to the transistor under test.

Appendix C

Noise studies should preferably be carried out in a screened room with well-filtered supplies and great care has to be taken to avoid spurious effects, hum and unreliable readings. The noise levels of interest are usually quite low so that high gain low-noise amplifiers are necessary to give the required sensitivity. In these circumstances quite a small degree of pick-up or interference can have unfortunate results. Hence it is a useful precaution to display the noise being measured on an oscilloscope.

In the elimination of hum, the first step is the determination of the hum frequency. 60 Hertz hum is due to direct electromagnetic pick up of the line frequency. It is eliminated by electromagnetic shielding and proper circuit layout. Shielding may be accomplished by surrounding the hum sensitive components with grounded metal screen.

Hum of 120 Hertz is usually due to ripple from the power supply (full wave rectifier) and is removed by better filtering. Hum at higher frequencies (360 Hertz , etc.) is caused by magnetic pickup from motors, transformers etc. Removal of it is often difficult and expensive. First, orientation of components should be tried followed by an additional shielding with mu-metal or other magnetic shielding materials.

Ground loops represent the most persistent, subtle, difficult-to-analyze and generally troublesome problem connected with power supply wiring. To avoid ground loop problems, it is absolutely

necessary to have only one ground return point in a power supply system, which includes the power supply and all its loads and all other power supplies connected to the same loads.

Hence, in the experimental setup the following steps were taken:

1. the test circuit was biased using batteries,
2. the test circuit was built inside a well shielded chassis, copper of thickness 1 mm,
3. the shielded chassis was made the ground return point for the entire system as shown in Fig. 3.2,
4. BNC Coaxial cables were used for all the external connections, and
5. finally the shielded chassis was oriented such that the noise monitored on the oscilloscope was a 'clean' noise, that is without any pickup.
6. The measured spectrum would indicate whether there was any anomalous behaviour over the frequency range. If abnormal behaviour is present, then there would be some sort of a bump in the $1/f$ region.

Appendix D

Measurement Accuracy

The measurement accuracy was affected by a number of factors and this is discussed below.

From equation (2.24), the equivalent noise power at the output is given by equation (D.1)

$$e_{\text{on}}^2 = 4KT_D R_n G_V^2 \Delta f \quad (\text{D.1})$$

Therefore, the error in R_n is given by equation (D.2)

$$\frac{\Delta R_n}{R_n} = \frac{2\Delta e_{\text{on}}}{e_{\text{on}}} + \frac{\Delta T}{T} + \frac{2\Delta G_V}{G_V} + \frac{\Delta(\Delta f)}{\Delta f} \quad (\text{D.2})$$

The collector current accuracy was within 2 percent and the collector-emitter voltage accuracy was within one percent.

The Delta Design oven MK 2300 was calibrated and the temperature measurement accuracy was $\pm 1^\circ\text{C}$, that is an error of less than half a percent was introduced by the temperature term in equation (D.2).

The signal generator in Fig. 3.1 was used for gain calibration and tuning purposes. The wave analyser, a Quantech model 303, was tuned to the signal generator frequency such that the frequency for gain calibration and spectrum analysis was one and the same. The accuracy of the tuned frequency of the wave analyser and the calibrated frequency (on the dial of wave analyser) was within 3 percent.

The voltage gain G_V of the system was determined by measuring input and output signals at the desired frequency on the HP 3400 voltmeter,

which is a 1 percent f.s.d. meter. The voltage gain ranged from 10^4 to 10^5 , depending on the operating conditions, and is known to within 2 percent.

The relative error of measurement $\sqrt{\alpha}$ for a linear detector is given by equation (D.3)

$$\sqrt{\alpha} = \frac{1}{2(\Delta f \tau)^{1/2}} \quad (D.3)$$

where τ is the time constant.

The bandwidth Δf has to be less than half the mid-frequency value and hence at low frequencies to increase the accuracy of measurement the time constant τ has to be increased from equation (D.3). A voltage integrator (R-C filter) was used to increase the time constant of the system from the 1 second value for the wave analyser meter to about 10 secs.

The bandwidth of the wave analyser was progressively increased with frequency. That is, at frequencies less than 60 Hz, the bandwidth used was 10 Hz; for the frequency range of 60 Hz to 200 Hz, the bandwidths used were 10 Hz and 30 Hz; for the frequency range of 200 Hz to 2 KHz, bandwidths used were 30 Hz and 100 Hz, and for frequencies above 2 KHz the bandwidths used were 100 Hz and 1000 Hz. The evaluation of R_n at a given frequency using different bandwidths gave consistent values, and the spread of R_n values obtained was about 2 percent above 200 Hz and about 4 percent below 200 Hz. The wave analyser bandwidth and the noise bandwidth were taken to be the same and the error introduced by this assumption in equation (D.2) was small compared to the error introduced by the gain term in equation (D.2).

The upper 3db frequency limitations of the test circuit was about 25 KHz. However, it was felt that extending measurements for frequencies above 20 KHz was not necessary as above the low frequency noise, the noise present would be white noise up to the α -cutoff frequency of the transistor.

Thus, at low frequencies the main source of error was due to excessive meter fluctuation as can be noted from equations (D.2) and (D.3).

Appendix E

Measurement of the Base Resistance

A brief review is given of some of the techniques available to determine the base resistance of a transistor. However, each method maybe applicable to only a particluar type of a BJT.

1. The low frequency value of $r_{b'b}(T)$ can be determined by using a common emitter hybrid-II model and measuring the short circuit input impedance h_{ie} .

$$h_{ie} \Big|_{1000\sim} = r_{b'b}(T) + r_{\pi} \quad (E.1)$$

$$r_{b'b}(T) = h_{ie} \Big|_{1000\sim} - r_{\pi} = h_{ie} \Big|_{1000\sim} - \frac{\beta_0}{g_m} \quad (E.2)$$

If the value of $r_{b'b}(T)$ is less than $r_{\pi}/10$, large errors in the determination of $r_{b'b}(T)$ may occur, resulting from the subtraction of two nearly equal numbers, h_{ie} and r_{π} . $r_{b'b}(T)$ is not independent of frequency and the value of the base resistance obtained by the low frequency method given above is not necessarily an appropriate value to use at higher frequencies, say, above 100 KHz.

2. This method² also makes use of the low frequency hybrid-II equivalent circuit. With a resistance in series with the base, the transconductance

$$G(j\omega) = \frac{g_m r_{\pi}}{R_s + r_{b'b}(T) + r_{\pi}} \quad (E.3)$$

is determined

$$G_1(j\omega) = \frac{g_m r_\pi}{R_s} \quad R_s \gg r_{b'b}(T) + r_\pi \quad (\text{E.4})$$

$$G_2(j\omega) = \frac{g_m r_\pi}{r_{b'b}(T) + r_\pi} \quad R_s \approx 0 \quad (\text{E.5})$$

Hence

$$r_{b'b}(T) = G_1(j\omega) R_s \left(\frac{1}{G_2(j\omega)} - \frac{1}{g_m} \right) \quad (\text{E.6})$$

$G_1(j\omega)$ and $G_2(j\omega)$ can be easily measured on a Wayne-Kerr autobalance universal bridge B641.

This method has the similar drawback of method 1.

3. In the frequency where the transistor shows significant flicker noise, it is often possible to adjust R_s so as to obtain a minimum in the emitter noise voltage. It can be shown^b that

$$R_{s(\text{min})} = \frac{KT}{q} \frac{1}{I_C} \cdot A - r_{b'b}(T) \quad (\text{E.7})$$

where A is some constant.

In order to obtain a minimum it is necessary that

$$\frac{r_e}{\alpha_0} > r_{b'b}(T) \quad (\text{E.8})$$

A large $r_{b'b}(T)$ would limit the current range over which a minimum results. That is, this method is applicable only to devices which have large 1/f noise levels and low base resistance, say 25 ohms.

A plot of the value of $R_{s(\text{min})}$ vs $\frac{KT}{qI_C}$ would intercept the R_s axis at $-r_{b'b}(T)$ and has slope A.

4. The collector output short circuit noise of a high gain transistor is given by²⁴

$$I_{eq} \approx \frac{\frac{2KT}{q} r_{b'b}(T) \beta_o^2}{\left(r_{b'b}(T) + \frac{\beta_o KT}{qI_C}\right)^2} \quad (E.9)$$

In the relatively small bias current region, $|I_C|$ less than 10 μA , the output noise is

$$I_{eq} = \frac{2q}{KT} r_{b'b}(T) I_C^2 \quad (E.10)$$

when

$$\frac{\beta_o KT}{qI_C} \gg r_{b'b}(T) \quad (E.11)$$

Therefore, in this region the output noise is proportional to the square of the d.c. collector current and is linearly proportional to the base resistance. The base resistance $r_{b'b}(T)$ can be determined from the slope of the plot of equation (E.10).

5. According to the hybrid- Π model, the base resistance can be obtained from a plot of the high frequency common-emitter input admittance, $|y_{ie}|$, versus frequency. If there is a plateau in the high frequency $|y_{ie}|$ data, then $|y_{ie}|$ in this region should be equal to $1/r_{b'b}(T)$. However, with many high-frequency transistors no such plateau exists, because the frequency response of the transistor has been improved to the point where the overlap-diode and header capacitance effects take over before $|y_{ie}|$ can level off to the value $1/r_{b'b}(T)$.

6. The base resistance of a microwave transistor can be measured by the power gain method²⁶. At very high frequency the input impedance Z_{be} of grounded emitter approaches $r_{b'b}(T)$

$$r_{b'b}(T) = \frac{G_1 - G_2}{\frac{G-G_1}{R_1} - \frac{G-G_2}{R_2}} \quad (\text{E.12})$$

where

$$G_i = \frac{f_t}{8\pi C_{ce}(r_{b'b}(T) + R_i) f^2} \quad i = 1, 2. \quad (\text{E.13})$$

and $G = G_i$ for $R_i = 0$.

G is the maximum power gain and G_1 and G_2 are the power gains with R_1 and R_2 in series with the base, respectively.

This is valid in the frequency range where β_0 falls at the rate of 6 db per octave, provided that feedback is negligible.

7. The base resistance of a microwave transistor can be determined by the input impedance method²⁶.

The input impedance of a grounded emitter transistor is measured over a wide range of frequencies and results plotted on a complex plane. The results give a semicircle and it is displayed from the origin by $r_{b'b}(T)$.

Appendix F

Current Gain β_0 of a Transistor

a.c. and d.c. current gain of a transistor can easily be measured on a Tektronix curve tracer of type 576.

β_0 is an increasing function of current at low current levels, as shown in Fig. F.1, because of the nonlinear effects in the base. In silicon devices the reason for this increase is that the tendency of added minority and majority carriers to recombine is progressively reduced as the total carrier concentrations involved are increased from their equilibrium values.

At high current levels, $I_c \geq 2$ mA, β_0 decreases with increasing current. The principal reason for this action stems directly from the increase of majority-carrier concentration in the base at high injection levels.

The strong variation of β_0 with temperature observed in Fig. E.1 is characteristic of silicon transistors and can be explained in the following way. It can be shown¹² that

$$\beta_0 = \frac{dI_{CF}}{dI_{BF}} = \frac{(dI_{CF})}{dq_{BF}} \frac{(dq_{BF})}{dI_{BF}} = \frac{\tau_{BF}}{\tau_F} \quad (F.1)$$

τ_F is the forward injection charge-control parameter and varies with temperature T only through D_b^{-1} , D_b gets smaller at higher temperatures. The increase of β_0 with temperature arises from τ_{BF} , the minority-carrier lifetime. In silicon, most of the recombination of

injected carriers takes place at imperfections or impurities (other than donors and acceptors) in the space-charge layer. At high temperatures, the rapid thermal motion of the carriers is thought to make their "capture" by such imperfections less probable, thus increasing τ_{BF} .

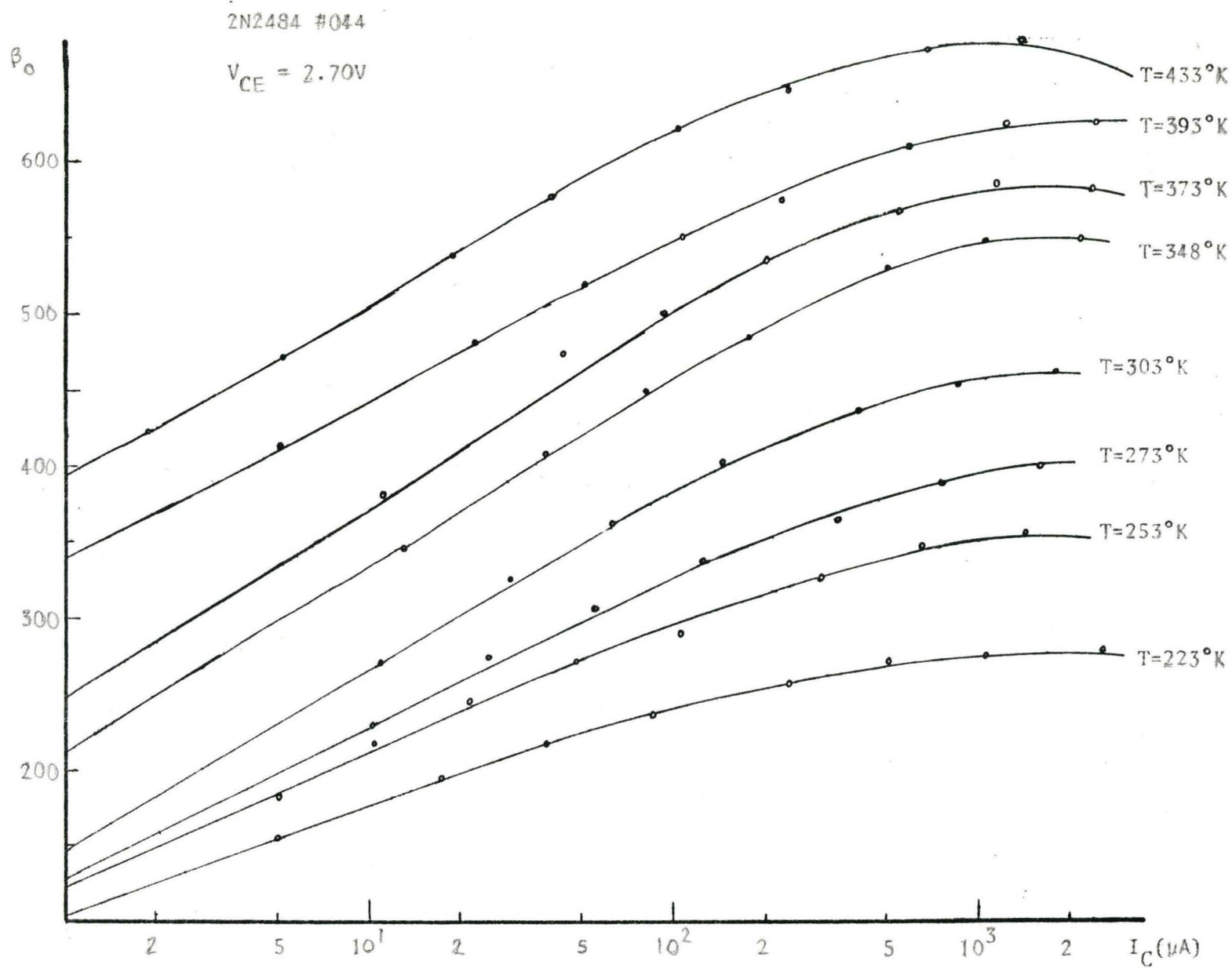


FIG. F.1 Current gain as a function of I_C with temperature as a parameter.